

# The $E_{\text{p},i} - E_{\text{iso}}$ correlation in GRBs: updated observational status, re-analysis and main implications

Lorenzo Amati<sup>1</sup>★

<sup>1</sup>INAF - IASF Bologna, via P. Gobetti 101, Bologna (Italy)

Submitted 2006 January 24.

## ABSTRACT

The correlation between the cosmological rest-frame  $\nu F_\nu$  spectrum peak energy,  $E_{\text{p},i}$ , and the isotropic equivalent radiated energy,  $E_{\text{iso}}$ , discovered by Amati et al. in 2002 and confirmed/extended by subsequent observations, is one of the most intriguing and debated observational evidences in Gamma-Ray Bursts (GRB) astrophysics. In this paper I provide an update and a re-analysis of the  $E_{\text{p},i} - E_{\text{iso}}$  correlation basing on an updated sample consisting of 41 long GRBs/XRFs with firm estimates of  $z$  and observed peak energy,  $E_{\text{p},\text{obs}}$ , 12 GRBs with uncertain values of  $z$  and/or  $E_{\text{p},\text{obs}}$ , 2 short GRBs with firm estimates of  $z$  and  $E_{\text{p},\text{obs}}$  and the peculiar sub-energetic events GRB980425/SN1998bw and GRB031203/SN2003lw. In addition to standard correlation analysis and power-law fitting, the data analysis here reported includes a modelization which accounts for sample variance. All 53 classical long GRBs and XRFs, including 11 *Swift* events with published spectral parameters and fluences, have  $E_{\text{p},i}$  and  $E_{\text{iso}}$  values, or upper/lower limits, consistent with the correlation, which shows a chance probability as low as  $\sim 7 \times 10^{-15}$ , a slope of  $\sim 0.57$  ( $\sim 0.5$  when fitting by accounting for sample variance) and an extra-Poissonian logarithmic dispersion of  $\sim 0.15$ , it extends over  $\sim 5$  orders of magnitude in  $E_{\text{iso}}$  and  $\sim 3$  orders of magnitude in  $E_{\text{p},i}$  and holds from the closer to the higher  $z$  GRBs. Sub-energetic GRBs (980425 and possibly 031203) and short GRBs are found to be inconsistent with the  $E_{\text{p},i} - E_{\text{iso}}$  correlation, showing that it can be a powerful tool for discriminating different classes of GRBs and understanding their nature and differences. I also discuss the main implications of the updated  $E_{\text{p},i} - E_{\text{iso}}$  correlation for the models of the physics and geometry of GRB emission, its use as a pseudo-redshift estimator and the tests of possible selection effects with GRBs of unknown redshift.

**Key words:** gamma-rays: observations – gamma-rays: bursts.

## 1 INTRODUCTION

Since 1997, with the first discoveries of optical counterparts and host galaxies, redshift estimates for Gamma-Ray Bursts (GRBs) have become available, allowing the study of the intrinsic properties of this challenging astrophysical phenomena. Among these, the correlation between the photon energy (commonly called *peak energy*) at which the cosmological rest frame  $\nu F_\nu$  spectrum peaks,  $E_{\text{p},i}$ , and the total isotropic-equivalent radiated energy,  $E_{\text{iso}}$ , is one of the most intriguing and discussed. This correlation was discovered by Amati et al. (2002) based on BeppoSAX data and subsequently confirmed and extended to X-Ray Rich GRBs (XRRs) and X-Ray Flashes (XRFs) based on HETE-2 data (Amati 2003; Lamb, Donaghy & Graziani 2004; Sakamoto et al. 2004, 2005a). It can be used to con-

strain the parameters of the various scenarios for the physics of GRB prompt emission, it is a challenging test for jet and GRB/XRF (X-Ray Flashes) unification models and it can provide hints on the nature of different sub-classes of GRBs (sub-energetic GRBs, short GRBs). Also, the  $E_{\text{p},i} - E_{\text{iso}}$  correlation has been used for building up redshift estimators and is frequently assumed as an input or as a required output for GRB population synthesis models. In this paper, I provide an update (up to December 2005) and a re-analysis of the  $E_{\text{p},i} - E_{\text{iso}}$  correlation based on a sample of a total of 56 events which includes *Swift* GRBs with known redshift and published spectral parameters and two very recent short GRBs with firm estimates of redshift and  $E_{\text{p},i}$ . The analysis here reported includes also fitting the data with a model which accounts for sample variance, given that this correlation is highly significant but also shows a dispersion which cannot be accounted for only by statistical fluctuations and is an important source of information. I also discuss the vari-

★ E-mail: amati@iasfbo.inaf.it

ous explanations and implications of the existence and properties of the  $E_{p,i} - E_{\text{iso}}$  correlation, its possible use for the estimate of pseudo-redshifts, and the tests based on GRBs with unknown redshift aimed to the evaluation of the impact of possible selection effects. For this last purpose, I also make use of published spectral parameters and fluences of a sample of 46 HETE-2 GRBs.

In order to introduce some basic information for the discussion reported in Section 5 and to allow a comparison between the results here reported and those reported in previous works, the description and properties of the updated sample (Section 3) the description and results of the data analysis results (Section 4) the discussion of the main implications and explanations of the  $E_{p,i} - E_{\text{iso}}$  correlation (Section 5) and the discussion of pseudo-redshift estimates and tests based on GRBs with unknown redshift (Section 6) are preceded (Section 2) by a brief review of spectral and energetics properties of GRBs and of previous studies of the  $E_{p,i} - E_{\text{iso}}$  correlation.

## 2 THE $E_{p,i} - E_{\text{iso}}$ CORRELATION

### 2.1 GRBs peak energy and radiated energy

The prompt emission spectra of GRBs are non thermal and in general can be modeled with the Band function (Band et al. 1993), a smoothly broken power-law whose parameters are the low energy spectral index,  $\alpha$ , the high energy spectral index,  $\beta$ , the break energy,  $E_0$ , and the overall normalization. In this model, if  $\beta < -2$  then the  $\nu F_\nu$  spectrum peak energy is given by  $E_{p,\text{obs}} = E_0 \times (2 + \alpha)$ . The spectral shape of most GRBs can be satisfactorily reproduced by Synchrotron Shock Models (SSM) (e.g. Tavani 1996): the kinetic energy of an ultra-relativistic fireball (a plasma made of pairs, photons and a small quantity of baryons) is dissipated into electromagnetic radiation by means of synchrotron emission originated in internal shocks between colliding shells and/or the external shock of the fireball with the ISM, see, e.g., Mészáros (2002) and Piran (2005) for recent reviews. Nevertheless, the time resolved analysis of BATSE and *BeppoSAX* GRBs showed that, at least during the initial phase of the emission, other mechanisms, like Compton up-scattering of UV photons surrounding the GRB source by the ultra relativistic electrons of the fireball or thermal emission by the photosphere of the fireball, may play an important role, see, e.g., Preece et al. (2000); Frontera et al. (2000b); Ghirlanda, Celotti & Ghisellini (2003). The latter emission mechanism could also be responsible for the smooth curvature characterizing GRB average spectra and, in particular, may determine the value of  $E_{p,\text{obs}}$  (Ryde 2005; Rees & Mészáros 2005). A relevant outcome of the analysis of BATSE events was the evidence of a substantial clustering of  $E_{p,\text{obs}}$  values around 200 keV, but in the recent years, the discovery and study of X-ray rich events and X-Ray Flashes (XRFs) by *BeppoSAX* and HETE-2, showed that the distribution of  $E_{p,\text{obs}}$  is much less clustered than inferred basing on BATSE data and, in particular, that it is characterized by a low energy tail extending down at least to  $\sim 1$  keV (Kippen et al. 2001; Sakamoto et al. 2005b).

Since the *BeppoSAX* breakthrough discoveries in 1997,

more than 70 redshift estimates have now become available. As a consequence, for these events it is possible to compute the intrinsic peak energy  $E_{p,i} = E_{p,\text{obs}} \times (1 + z)$  and the radiated energy in a given cosmological rest-frame energy band following, e.g., the methods described in Amati et al. (2002), Amati (2003) and Ghirlanda, Ghisellini & Lazzati (2004). In the simplest assumption of isotropic emission, the radiated energy,  $E_{\text{iso}}$ , ranges from  $\sim 10^{50}$  erg to  $\sim 10^{54}$  erg for most GRBs and extends down to  $\sim 10^{49}$  erg when including XRFs (Lamb, Donaghy & Graziani 2004; Sakamoto et al. 2004). When assuming that the GRB emission is jet-like, based on achromatic breaks observed in the afterglow decay curves of several GRBs, the distribution of the collimation corrected radiated energy,  $E_\gamma$ , was initially found to be clustered around  $\sim 10^{51}$  erg (Frail et al. 2001; Bloom, Frail & Kulkarni 2003); however, recently Ghirlanda, Ghisellini & Lazzati (2004) showed that, when considering a larger sample of GRBs with known redshift, the  $E_\gamma$  distribution is broader than inferred before.

### 2.2 Discovery, confirmation and extension of the $E_{p,i} - E_{\text{iso}}$ correlation

In 2002, Amati et al. (2002) presented the results of the analysis of the average 2–700 keV spectra of 12 *BeppoSAX* GRBs with known redshift (9 firm measurements and 3 possible values). The more relevant outcome of this work was the evidence of a strong correlation between  $E_{p,i}$  and  $E_{\text{iso}}$ . The linear correlation coefficient between  $\log(E_{p,i})$  and  $\log(E_{\text{iso}})$  was found to be 0.949 for the 9 GRBs with firm redshift estimates, corresponding to a chance probability of  $\sim 0.005\%$ . The slope of the power-law best describing the trend of  $E_{p,i}$  as a function of  $E_{\text{iso}}$  was  $\sim 0.5$ . This work was extended by Amati (2003) by including in the sample 10 more events with known redshift for which new spectral data (*BeppoSAX* events) or published best fit spectral parameters (BATSE and HETE-2 events) were available. The  $E_{p,i} - E_{\text{iso}}$  correlation was confirmed and its significance increased, giving a correlation coefficient similar to that derived by Amati et al. (2002) but with a much higher number of events. Basing on HETE-2 measurements, Lamb, Donaghy & Graziani (2004), Sakamoto et al. (2004) and Sakamoto et al. (2005a) not only confirmed the  $E_{p,i} - E_{\text{iso}}$  correlation but remarkably extended it to XRFs, showing that it holds over three orders of magnitude in  $E_{p,i}$  and five orders of magnitude in  $E_{\text{iso}}$ . The addition of new data, as more redshift estimates became available, confirmed the correlation and increased its significance, as found e.g. by Ghirlanda, Ghisellini & Lazzati (2004) (29 events, chance probability of  $7.6 \times 10^{-7}$ ). Finally, the relevance of the  $E_{p,i} - E_{\text{iso}}$  correlation for the GRB field stimulated several similar studies, which led to the discovery of correlations of  $E_{p,i}$  with other GRB intensity indicators like the average isotropic equivalent luminosity  $L_{\text{iso}}$  (Lamb, Donaghy & Graziani 2004, 2005) and the peak isotropic equivalent luminosity  $L_{p,\text{iso}}$  (Yonetoku et al. 2004; Ghirlanda et al. 2005a). Liang, Dai & Wu (2004) also showed that, at least for a good fraction of events, the  $E_{p,i} - L_{\text{iso}}$  correlation holds also within GRBs. All these correlations show the same slope and dispersion of the  $E_{p,i} - E_{\text{iso}}$  correlation, and reflect the tight correlation existing between  $E_{\text{iso}}$ ,  $L_{\text{iso}}$  and  $L_{p,\text{iso}}$  (Lamb, Donaghy & Graziani

**Table 1.**  $E_{\text{p,i}}$  and  $E_{\text{iso}}$  values for long GRBs and XRFs with firm estimates of both  $z$  and  $E_{\text{p,obs}}$  (41 events), the peculiar sub-energetic event GRB980425 and the only two short GRBs with firm estimates of  $z$  and  $E_{\text{p,obs}}$ , GRB050709 and GRB051221. The uncertainties are at  $1\sigma$  significance. The "Type" column indicates whether the event is a normal long GRB (LONG), an X-Ray Flash (XRF) or is sub-energetic (SUB-EN). The "Instruments" column reports the name of the experiment(s), or of the satellite(s), that provided the estimates of spectral parameters and fluence (BAT = BATSE, SAX = *BeppoSAX*, HET = HETE-2, KON = Konus, SWI = *Swift*). The last two columns report the references for the spectral parameters and the references for the values and uncertainties of  $E_{\text{iso}}$ , respectively. The "—" sign indicates that  $E_{\text{iso}}$  was computed specifically for this work (see text). GRBs detected by *Swift* are marked with an asterisk.

| GRB      | Type   | $z$    | $E_{\text{p,i}}$<br>(keV)     | $E_{\text{iso}}$<br>( $10^{52}$ erg) | Instruments | Refs. for (a)<br>spectrum | Refs. for (a)<br>$E_{\text{iso}}$ |
|----------|--------|--------|-------------------------------|--------------------------------------|-------------|---------------------------|-----------------------------------|
| 970228   | LONG   | 0.695  | 195 $\pm$ 64                  | 1.86 $\pm$ 0.14                      | SAX         | (1)                       | (1)                               |
| 970508   | LONG   | 0.835  | 145 $\pm$ 43                  | 0.71 $\pm$ 0.15                      | SAX         | (1)                       | (1)                               |
| 970828   | LONG   | 0.958  | 586 $\pm$ 117                 | 34 $\pm$ 4                           | BAT         | (2)                       | (3)                               |
| 971214   | LONG   | 3.42   | 685 $\pm$ 133                 | 24 $\pm$ 3                           | SAX         | (1)                       | (1)                               |
| 980425   | SUB-EN | 0.0085 | 55 $\pm$ 21                   | 0.00010 $\pm$ 0.00002                | BAT         | (4)                       | (4)                               |
| 980613   | LONG   | 1.096  | 194 $\pm$ 89                  | 0.68 $\pm$ 0.11                      | SAX         | (1)                       | (1)                               |
| 980703   | LONG   | 0.966  | 503 $\pm$ 64                  | 8.3 $\pm$ 0.8                        | BAT         | (2)                       | (3)                               |
| 990123   | LONG   | 1.60   | 1724 $\pm$ 466 <sup>(b)</sup> | 266 $\pm$ 43                         | SAX/BAT/KON | (1,2,5)                   | (1,5)                             |
| 990506   | LONG   | 1.30   | 677 $\pm$ 156 <sup>(b)</sup>  | 109 $\pm$ 11                         | BAT/KON     | (2,5)                     | (3,5)                             |
| 990510   | LONG   | 1.619  | 423 $\pm$ 42                  | 20 $\pm$ 3                           | SAX         | (1)                       | (1)                               |
| 990705   | LONG   | 0.842  | 459 $\pm$ 139 <sup>(b)</sup>  | 21 $\pm$ 3                           | SAX/KON     | (1)                       | (1)                               |
| 990712   | LONG   | 0.434  | 93 $\pm$ 15                   | 0.78 $\pm$ 0.15                      | SAX         | (1)                       | (1)                               |
| 991208   | LONG   | 0.706  | 313 $\pm$ 31                  | 25.9 $\pm$ 2.1                       | KON         | (5)                       | (5)                               |
| 991216   | LONG   | 1.02   | 648 $\pm$ 134 <sup>(b)</sup>  | 78 $\pm$ 8                           | BAT/KON     | (2)                       | (3)                               |
| 000131   | LONG   | 4.50   | 987 $\pm$ 416 <sup>(b)</sup>  | 199 $\pm$ 35                         | BAT/KON     | (5)                       | (5)                               |
| 000210   | LONG   | 0.846  | 753 $\pm$ 26                  | 17.3 $\pm$ 1.9                       | KON         | (5)                       | (5)                               |
| 000418   | LONG   | 1.12   | 284 $\pm$ 21                  | 10.6 $\pm$ 2.0                       | KON         | (5)                       | (5)                               |
| 000911   | LONG   | 1.06   | 1856 $\pm$ 371 <sup>(c)</sup> | 78 $\pm$ 16                          | KON         | (6)                       | (6)                               |
| 000926   | LONG   | 2.07   | 310 $\pm$ 20                  | 31.4 $\pm$ 6.8                       | KON         | (5)                       | (5)                               |
| 010222   | LONG   | 1.48   | 766 $\pm$ 30                  | 94 $\pm$ 10                          | KON         | (5)                       | (5)                               |
| 010921   | LONG   | 0.450  | 129 $\pm$ 26                  | 1.10 $\pm$ 0.11                      | HET         | (8)                       | (3)                               |
| 011211   | LONG   | 2.14   | 186 $\pm$ 24                  | 6.3 $\pm$ 0.7                        | SAX         | (3)                       | (3)                               |
| 020124   | LONG   | 3.20   | 448 $\pm$ 148 <sup>(b)</sup>  | 31 $\pm$ 3                           | HET/KON     | (8,5)                     | (3)                               |
| 020813   | LONG   | 1.25   | 590 $\pm$ 151 <sup>(b)</sup>  | 76 $\pm$ 19 <sup>(b)</sup>           | HET/KON     | (5,7)                     | (3,5)                             |
| 020819b  | LONG   | 0.410  | 70 $\pm$ 21                   | 0.79 $\pm$ 0.20                      | HET         | (8)                       | —                                 |
| 020903   | XRF    | 0.250  | 3.37 $\pm$ 1.79               | 0.0028 $\pm$ 0.0007                  | HET         | (9)                       | (9)                               |
| 021004   | LONG   | 2.30   | 266 $\pm$ 117                 | 3.8 $\pm$ 0.5                        | HET         | (8)                       | (26)                              |
| 021211   | LONG   | 1.01   | 127 $\pm$ 52 <sup>(b)</sup>   | 1.3 $\pm$ 0.15                       | HET/KON     | (5,10)                    | (5,13)                            |
| 030226   | LONG   | 1.98   | 289 $\pm$ 66                  | 14 $\pm$ 1.5                         | HET         | (8)                       | (13)                              |
| 030328   | LONG   | 1.52   | 328 $\pm$ 55                  | 43 $\pm$ 4                           | HET/KON     | (5,8)                     | —                                 |
| 030329   | LONG   | 0.17   | 100 $\pm$ 23 <sup>(b)</sup>   | 1.7 $\pm$ 0.3 <sup>(b)</sup>         | HET/KON     | (5,8)                     | —                                 |
| 030429   | LONG   | 2.65   | 128 $\pm$ 26                  | 2.50 $\pm$ 0.30                      | HET         | (8)                       | (26)                              |
| 040924   | LONG   | 0.859  | 102 $\pm$ 35 <sup>(b)</sup>   | 1.1 $\pm$ 0.12                       | HET/KON     | (14,28)                   | (27)                              |
| 041006   | LONG   | 0.716  | 98 $\pm$ 20                   | 3.5 $\pm$ 1.0                        | HET         | (29)                      | —                                 |
| 050318*  | LONG   | 1.44   | 115 $\pm$ 25                  | 2.55 $\pm$ 0.18                      | SWI         | (16)                      | (16)                              |
| 050401*  | LONG   | 2.90   | 467 $\pm$ 110                 | 41 $\pm$ 8                           | KON         | (17)                      | (17)                              |
| 050416a* | XRF    | 0.650  | 25.1 $\pm$ 4.2                | 0.12 $\pm$ 0.02                      | SWI         | (19)                      | (19)                              |
| 050525*  | LONG   | 0.606  | 127 $\pm$ 10                  | 3.39 $\pm$ 0.17                      | SWI         | (20)                      | —                                 |
| 050603*  | LONG   | 2.821  | 1333 $\pm$ 107                | 70 $\pm$ 5                           | KON         | (21)                      | —                                 |
| 050709   | SHORT  | 0.16   | 100 $\pm$ 16                  | 0.0103 $\pm$ 0.0021                  | HET         | (18)                      | (18)                              |
| 050922c* | LONG   | 2.198  | 415 $\pm$ 111                 | 6.1 $\pm$ 2.0                        | HET         | (22)                      | (22)                              |
| 051022*  | LONG   | 0.80   | 754 $\pm$ 258 <sup>(b)</sup>  | 63 $\pm$ 6                           | HET/KON     | (23,30)                   | —                                 |
| 051109*  | LONG   | 2.346  | 539 $\pm$ 200                 | 7.5 $\pm$ 0.8                        | KON         | (24)                      | —                                 |
| 051221*  | SHORT  | 0.5465 | 622 $\pm$ 35                  | 0.29 $\pm$ 0.06                      | KON         | (25)                      | (25)                              |

Notes. (a) References for the spectral parameters and for the values and uncertainties of  $E_{\text{p,i}}$  and  $E_{\text{iso}}$ : (1) Amati et al. (2002), (2) Jimenez, Band & Piran (2001), (3) Amati (2003), (4) Yamazaki, Yonetoku & Nakamura (2003), (5) Ulanov et al. (2005), (6) Price et al. (2002), (7) Barraud et al. (2003), (8) Sakamoto et al. (2005b), (9) Sakamoto et al. (2004), (10) Crew et al. (2003), (11) Atteia (2003), (12) Atteia et al. (2005), (13) Ghirlanda, Ghisellini & Lazzati (2004), (14) Golenetskii et al. (2004), (15) Friedman & Bloom (2005), (16) Perri et al. (2005), (17) Golenetskii et al. (2005a), (18) Villasenor et al. (2005), (19) Sakamoto et al. (2005a), (20) Cummings et al. (2005), (21) Golenetskii et al. (2005b), (22) Crew et al. (2005a), (23) Golenetskii et al. (2005c), (24) Golenetskii et al. (2005d), (25) Golenetskii et al. (2005e), (26) Friedman & Bloom (2005), (27) Ghirlanda et al. (2005b), (28) Fenimore et al. (2004), (29) Official HETE GRB page (<http://space.mit.edu/HETE/Bursts/>), (30) Doty et al. (2005) <sup>(b)</sup> Uncertainties enlarged in order to account for significantly different values measured by different instruments (see text). <sup>(c)</sup> Value derived from time resolved spectral analysis by weighting each time interval with the ratio between its fluence and the total GRB fluence. A 20% error is conservatively assumed.

**Table 2.**  $E_{p,i}$  and  $E_{iso}$  values for GRBs and XRFs with uncertain estimates, or upper / lower limits, of  $z$  or  $E_{p,obs}$ . The uncertainties are at  $1\sigma$  significance, whereas the upper/lower limits are at 90% c.l. The "Type" column indicates whether the event is a normal long GRB (LONG), an X-Ray Flash (XRF) or is sub-energetic (SUB-EN). The "Instruments" column reports the name of the experiment(s), or of the satellite(s), that provided the estimates or upper/lower limit to the spectral parameters and of the fluence (BAT = BATSE, SAX = *BepoSAX* , HET = HETE-2, KON = Konus, SWI = *Swift* ). The last two columns report the references for the spectral parameters and the references for the values and uncertainties (or upper / lower limits) of  $E_{iso}$  , respectively. The "–" sign indicates that  $E_{iso}$  was computed specifically for this work (see text). GRBs detected by *Swift* are marked with an asterisk.

| GRB     | Type   | $z$         | $E_{p,i}$<br>(keV)  | $E_{iso}$<br>( $10^{52}$ erg) | Instruments | Refs. for <sup>(a)</sup><br>spectrum | Refs. for <sup>(a)</sup><br>$E_{iso}$ |
|---------|--------|-------------|---------------------|-------------------------------|-------------|--------------------------------------|---------------------------------------|
| 980326  | LONG   | 1.0         | $71 \pm 36$         | $0.56 \pm 0.11$               | SAX         | (1)                                  | (1)                                   |
| 980329  | LONG   | $2.0-3.9$   | $935 \pm 150$       | $177 \pm 58^{(b)}$            | SAX         | (1)                                  | (1,12)                                |
| 981226  | LONG   | 1.11        | $<160^{(c)}$        | $0.59 \pm 0.12$               | SAX         | (13)                                 | –                                     |
| 000214  | LONG   | $0.37-0.47$ | $>117$              | $0.93 \pm 0.03$               | SAX         | (1)                                  | (1)                                   |
| 001109  | LONG   | 0.40        | $101 \pm 45$        | $0.40 \pm 0.02$               | SAX         | (3)                                  | –                                     |
| 011121  | LONG   | 0.360       | $793 \pm 533^{(b)}$ | $9.9 \pm 2.2^{(b)}$           | SAX/KON     | (7,11)                               | (7,11)                                |
| 020405  | LONG   | 0.69        | $612 \pm 122$       | $12.8 \pm 1.5$                | SAX         | (4)                                  | (5)                                   |
| 030323  | LONG   | 3.37        | $270 \pm 113$       | $3.2 \pm 1.0$                 | HET         | (12)                                 | (27)                                  |
| 030723  | XRF    | $<2.3$      | $<0.023$            | $<16.$                        | HET         | (6)                                  | (5)                                   |
| 031203  | SUB-EN | 0.105       | $158 \pm 51$        | $0.010 \pm 0.004$             | KON         | (7)                                  | (7,14)                                |
| 050315* | LONG   | 1.949       | $<89$               | $4.9 \pm 1.5$                 | SWI         | (8)                                  | (8)                                   |
| 050824* | LONG   | 0.83        | $<23$               | $0.130 \pm 0.029$             | HET         | (9)                                  | –                                     |
| 050904* | LONG   | 6.29        | $>1100$             | $193 \pm 127$                 | SWI         | (10)                                 | (10)                                  |

Notes. <sup>(a)</sup>References for the spectral parameters and for the values and uncertainties of  $E_{p,i}$  and  $E_{iso}$  : (1) Amati et al. (2002), (2) Christensen, Hjorth & Gorosabel (2005), (3) Amati et al. (2003b), (4) Price et al. (2003), (5) Ghirlanda, Ghisellini & Lazzati (2004), (6) Sakamoto et al. (2005b), (7) Ulanov et al. (2005), (8) Vaughan et al. (2006), (9) Crew et al. (2005b), (10) Cusumano et al. (2006), (11) Amati (2003), (12) Jimenez, Band & Piran (2001), (13) Frontera et al. (2000a), (14) Sazonov, Lutovinov & Sunyaev (2004) <sup>(b)</sup> Uncertainties enlarged in order to account for significantly different values measured by different instruments (see text). <sup>(c)</sup> Upper limit inferred from time resolved spectral analysis.

2004, 2005; Ghirlanda et al. 2005a). More intriguing, as will be discussed in Section 5, are the  $E_{p,i} - E_{\gamma}$  and  $E_{p,i} - E_{iso} - t_b$  ( $t_b$  is the achromatic afterglow light curve break time) correlations discovered by Ghirlanda, Ghisellini & Lazzati (2004) and Liang & Zhang (2005) basing on a limited sample of GRBs with known  $z$ ,  $E_{p,i}$  and  $t_b$ . Also, evidence of a strong correlation between  $E_{p,i}$ ,  $E_{iso}$  and the "high-signal" time scale  $T_{0.45}$  has been found very recently (Firmani et al. 2006).

The outcome of the analysis of the  $E_{p,i} - E_{iso}$  correlation performed in previous works are summarized in the first five lines of Table 3. As it can be seen, the chance probability of this correlation is very low and decreases when increasing the number of events in the sample considered. Nevertheless, the fits with a power-law are always very poor (as indicated by the reported  $\chi^2$  values) and both the normalization and the index vary significantly depending on the sample considered. This is an effect of the extra-Poissonian dispersion of the correlation, as will be discussed in detail in the next Section.

### 3 UPDATED SAMPLE AND DISTRIBUTIONS OF $E_{p,i}$ AND $E_{iso}$ .

The last three lines of Table 3 report the results of the analysis that I performed on the most updated (as of December 2005) sample of long GRBs/XRFs with firm estimates of both  $z$  and  $E_{p,obs}$  . This sample, reported in Table 1, consists of a total of 41 events and includes

events already considered in previous works, new events, such as *Swift* GRBs, and older events for which useful spectral information has become available only recently, as is the case e.g. for some events detected by Konus/Wind (Ulanov et al. 2005). Table 1 includes also the peculiar sub-energetic event GRB980425 and the only two short GRBs (GRB050709 and GRB051221) for which firm estimates of  $z$  and  $E_{p,obs}$  are available. Table 2 includes 12 classical long GRBs and the other sub-energetic event GRB031203, with uncertain estimates of  $z$  or  $E_{p,obs}$  . It also includes XRF030723, for which only an upper limit to the redshift is available. The  $E_{p,i}$  and  $E_{iso}$  values of more than half of the events are taken from Amati et al. (2002), Amati (2003), Ghirlanda, Ghisellini & Lazzati (2004), Friedman & Bloom (2005), Ulanov et al. (2005), while for the other events they are taken from specific references, mostly GCNs. For HETE-2 GRBs with estimates of  $E_{p,obs}$  available from both Barraud et al. (2003) and Sakamoto et al. (2005a), I used the values from Sakamoto et al. (2005a), which are based on joint WXM/FREGATE analysis. The only exception to this rule is GRB020813, for which a depletion of X-ray photons in the WXM energy band was observed by means of time resolved spectral analysis (Sato et al. 2005a). Some GRBs included in the samples of some of the works mentioned above, were excluded from the sample of GRBs with firm estimates of  $z$  and  $E_{p,i}$  because of a too large difference between the  $E_{p,obs}$  measured by different detectors (e.g. GRB011121) or a poorly unconstrained 90% c.l. interval of  $E_{p,obs}$  (e.g. GRB030323) (see references in Table 2). For

all GRBs, the last two columns of Tables 1 and 2 report the references for the spectral parameters and for the values and uncertainties of  $E_{\text{p},\text{i}}$  and  $E_{\text{iso}}$ , including also the methods adopted to derive these quantities based on the measured spectra and fluences. It has to be noted that in the computation of  $E_{\text{iso}}$  some authors assume  $H_0=65 \text{ km s}^{-1} \text{ Mpc}^{-1}$  (e.g., Amati et al. 2002), while others assume  $H_0=70 \text{ km s}^{-1} \text{ Mpc}^{-1}$  (e.g., Ghirlanda, Ghisellini & Lazzati 2004); instead, the values of  $\Omega_m$  and  $\Omega_\Lambda$  are always assumed to be 0.3 and 0.7, respectively. Thus, in order to have a homogeneous data set, I corrected the  $E_{\text{iso}}$  values computed by assuming  $H_0=70 \text{ km s}^{-1} \text{ Mpc}^{-1}$  by accounting for the different luminosity distance obtained with  $H_0=65 \text{ km s}^{-1} \text{ Mpc}^{-1}$ .

The  $E_{\text{iso}}$  values from Ulanov et al. (2005) were computed by integrating the observed fluence between  $10/(1+z)$  and  $10000/(1+z)$  keV (Ulanov, private communication) and thus between 10–10000 keV in the GRB cosmological rest-frame. The difference with respect to integrating from 1 to 10000 keV clearly depends on the spectral parameters, in particular on  $\alpha$ , and is not higher than 10% in the worst cases (and typically of the order of 3–5%). Given that the values of  $\alpha$  are not reported by Ulanov et al. (2005), I corrected their  $E_{\text{iso}}$  values and  $1\sigma$  confidence intervals by conservatively assuming that the extension of the integration from 10 keV to 1 keV may contribute from 0 to 10% to the total radiated energy.

For some events of the sample, marked with a note in Tables 1 and 2, I enlarged the uncertainties on  $E_{\text{p},\text{i}}$  and/or  $E_{\text{iso}}$  in order to include the different central values and  $1\sigma$  uncertainties reported in the literature based on measurements by different GRB detectors. The issue of the systematics in the estimates of spectral parameters and fluence due to detectors limited energy bands and sensitivities as a function of photon energy is discussed in Sections 5.3 and 6.2. For those few events for which there is no reference directly reporting the values of  $E_{\text{p},\text{i}}$  and/or  $E_{\text{iso}}$ , these have been calculated based on published spectral parameters and fluence by following the methods mentioned in previous Section and detailed e.g. in Amati et al. (2002) and Ghirlanda, Ghisellini & Lazzati (2004). In particular, the unpublished values of  $E_{\text{iso}}$  have been computed in the 1–10000 keV cosmological rest-frame energy band and by assuming a standard cosmology with  $\Omega_m=0.3$ ,  $\Omega_\Lambda=0.7$  and  $H_0=65 \text{ km s}^{-1} \text{ Mpc}^{-1}$ . For these events, the uncertainties on  $E_{\text{p},\text{i}}$  and  $E_{\text{iso}}$  were computed by propagating the fractional errors on  $E_0$  and fluence, respectively, as done, e.g., in Amati (2003) for BATSE and HETE-2 events. The values of  $z$  have been taken directly from J. Greiner's GRB Table<sup>1</sup>, which also includes complete references. For those cases in which only a range for  $z$  is available (Table 2),  $E_{\text{p},\text{i}}$  and  $E_{\text{iso}}$  have been computed by assuming the central value. In the case of XRF030723 (Table 2), the upper limit to the redshift comes from Fynbo et al. (2004) and the upper limits to  $E_{\text{p},\text{i}}$  and  $E_{\text{iso}}$  from Lamb, Donaghy & Graziani (2004).

It is important to notice that GRBs included in these samples have been detected, and their spectral parameters measured, by detectors with different sensitivities and energy bands. This, together with the fact that *Swift* is allow-

ing  $z$  determinations for more types of GRBs, should reduce significantly the possible impact of selection effects. This issue will be discussed in Section 6.

In Figure 1 I show the logarithmic distributions of  $E_{\text{iso}}$  (left panel) and  $E_{\text{p},\text{i}}$  (right panel). These refer to all the GRBs included in Table 1 plus GRB031203 (Table 2). As can be seen, in both cases the bulk of the distribution can be fitted by a Gaussian, but a low energy tail is evident. In the  $\log(E_{\text{iso}})$  distribution, the low tail is due to the sub-energetic GRBs 980425 and 031203, the XRF 020903 and the short GRB 050709; the fit of this distribution with a Gaussian gives an average of  $\sim 10^{53}$  erg and a logarithmic dispersion of  $\sim 0.9$ . It is noticeable that the  $E_{\text{iso}}$  distribution spans about 6 orders of magnitude. The fit of the  $\log(E_{\text{p},\text{i}})$  distribution with a Gaussian gives an average of  $\sim 350$  keV and a logarithmic dispersion of  $\sim 0.45$ . In this case the low-energy tail is given by the XRFs 020903 and 050416a, while sub-energetic and short GRBs show  $E_{\text{p},\text{i}}$  values consistent with the bulk of the distribution. It is worthing to note that the  $E_{\text{p},\text{i}}$  distribution is much broader than the  $E_{\text{p},\text{obs}}$  distribution inferred from BATSE GRBs (Kaneko et al. 2006).

#### 4 THE $E_{\text{p},\text{i}} - E_{\text{iso}}$ CORRELATION: RE-ANALYSIS

The  $(E_{\text{p},\text{i}}, E_{\text{iso}})$  points corresponding to the 41 GRBs/XRFs with with firm estimates of  $z$  and  $E_{\text{p},\text{i}}$ , all included in Table 1, are shown in Figure 2, whereas the  $(E_{\text{p},\text{i}}, E_{\text{iso}})$  points and upper/lower limits corresponding to the GRBs with uncertain  $z$  and  $E_{\text{p},\text{i}}$  (Table 2) are shown in Figure 3, which also includes the points corresponding to the peculiar sub-energetic GRB980425 and the two short GRBs 050709 and 051221. In both Figures, the point corresponding to *Swift* GRBs are shown as filled circles. The first two lines of the second part of Table 3 report the results of the analysis performed on the sample plotted in Figure 2. The correlation analysis is based on the estimate of the Spearman's rank correlation coefficient between  $E_{\text{p},\text{i}}$  and  $E_{\text{iso}}$  and the fits with a power-law  $E_{\text{p},\text{i}} = K \times E_{\text{iso}}^m$  are performed by accounting for the errors on both  $E_{\text{p},\text{i}}$  and  $E_{\text{iso}}$ . As can be seen, with the updated sample subject of this analysis, the chance probability of correlation between the logarithms of  $E_{\text{p},\text{i}}$  and  $E_{\text{iso}}$  is as low as  $\sim 3.5 \times 10^{-14}$ , when considering only the 41 classical GRBs, and  $\sim 10^{-14}$  when including also the XRFs 020903 and 050416a. Thus, increasing the sample by adding new data and making it more complete (as mentioned above) not only confirms the  $E_{\text{p},\text{i}} - E_{\text{iso}}$  correlation but also reduces its chance probability to a negligible value. The index of the power-law,  $\sim 0.57$ , is found to lie in the range 0.4–0.6, consistently with the findings of previous analysis, and does not change significantly by including or not in the sample XRFs 020903 and 050416a (see Table 3). The value of the normalization is found to be somewhat lower with respect to previous analysis, except for the recent analysis performed by Nava et al. (2006) on a subsample of 18 GRBs which includes more recent events with respect to previous works. The power-law best fitting the data of the 41 GRBs with firm estimates of  $z$  and  $E_{\text{p},\text{i}}$  is shown as a dashed line in Figures 2 and 3.

Despite the correlation is very highly significant, the  $\chi^2$  values obtained by fitting the data with a power-law are

<sup>1</sup> <http://www.mpe.mpg.de/~jcg/grbgen.html>

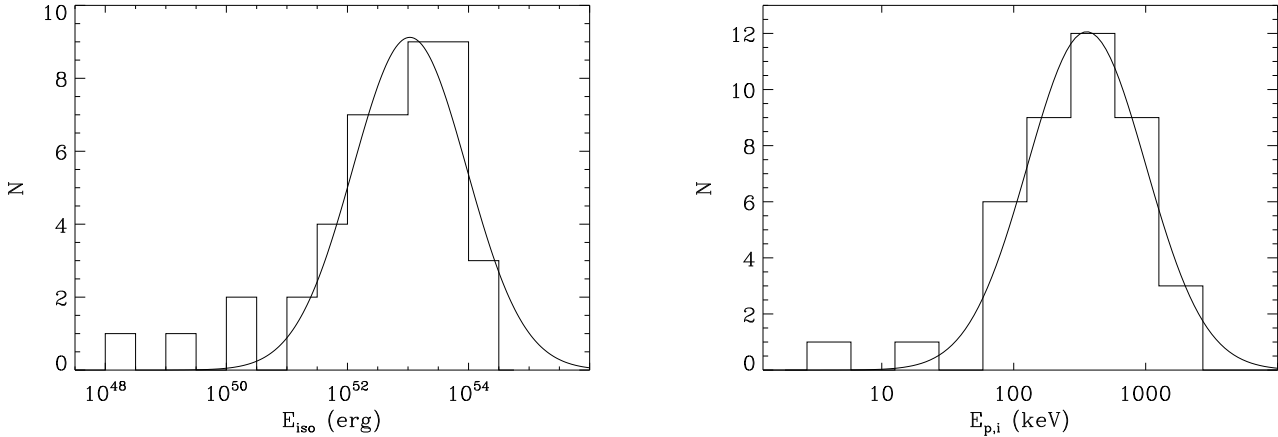


**Figure 1.** Distributions of  $\log(E_{\text{iso}})$  (left) and  $\log(E_{\text{p},i})$  (right) for the 41 GRBs with firm redshift and  $E_{\text{p,obs}}$ , the short GRBs 050709 and 051221 and the sub-energetic GRBs 980425 and 031203. For both distributions, the best fit Gaussian is superimposed to the data.

**Table 3.** Summary of the results of the analysis of the  $E_{\text{p},i} - E_{\text{iso}}$  correlation as reported in previous works (top) and performed in this work (bottom). The coefficient  $\rho$  is the Spearman's rank correlation coefficient between  $E_{\text{p},i}$  and  $E_{\text{iso}}$ . N is the number of events considered, m, K and  $\chi^2_{\nu}$  refer to fits of the  $E_{\text{p},i} - E_{\text{iso}}$  correlation with a power-law  $E_{\text{p},i} = K \times E_{\text{iso}}^m$  ( $E_{\text{p},i}$  is in keV and  $E_{\text{iso}}$  in units of  $10^{52}$  erg). The uncertainties reported in the first part of the Table (values taken from the literature) are at  $1\sigma$  confidence level, while those reported in the second part (results obtained in this work) are at 90% significance. When not available in the literature, the values of K and  $\chi^2_{\nu}$  reported in the top part of the Table have been computed specifically for this work.

| Reference                                    | N  | $\rho$ | Chance Prob.          | m                      | K               | $\chi^2_{\nu}$ |
|--|----|--------|-----------------------|------------------------|-----------------|----------------|
| Amati et al. (2002)                          | 9  | 0.92   | $5.0 \times 10^{-4}$  | $0.52 \pm 0.06$        | $105 \pm 11$    | 3.9            |
| Amati (2003)                                 | 20 | 0.92   | $1.1 \times 10^{-8}$  | $0.35 \pm 0.06$        | $118 \pm 9$     | 6.1            |
| Ghisellini, Ghirlanda & Lazzati (2004)       | 27 | 0.80   | $7.6 \times 10^{-7}$  | $0.40 \pm 0.05$        | $95 \pm 7$      | 6.2            |
| Friedman & Bloom (2005)                      | 29 | 0.88   | $4.9 \times 10^{-10}$ | $0.50 \pm 0.04$        | $90 \pm 8$      | 9.5            |
| Nava et al. (2006)                           | 18 | 0.82   | $3.1 \times 10^{-5}$  | $0.57 \pm 0.02$        | $71 \pm 2$      | 5.2            |
| This work (only GRBs)                        | 39 | 0.89   | $3.1 \times 10^{-14}$ | $0.57^{+0.02}_{-0.02}$ | $80^{+4}_{-4}$  | 7.2            |
| This work (including XRFs 020903 and 050416) | 41 | 0.89   | $7.0 \times 10^{-15}$ | $0.57^{+0.02}_{-0.02}$ | $81^{+2}_{-2}$  | 6.9            |
| This work (accounting for sample variance)   | 41 | 0.89   | $7.0 \times 10^{-15}$ | $0.49^{+0.06}_{-0.05}$ | $95^{+11}_{-9}$ | 0.95           |

poor, as found in previous analysis (Table 3). This means that the scatter of the data around the best fit model cannot be due only to statistical fluctuations, unless the systematics in the estimates of  $E_{\text{p},i}$  and  $E_{\text{iso}}$  are strongly underestimated, as will be discussed in next Section. Another effect of the dispersion characterizing the correlation is that, as mentioned above, the slope and normalization of the power-law are found to change significantly depending on the sub-sample considered. This extra-Poissonian dispersion of the  $E_{\text{p},i} - E_{\text{iso}}$  correlation, which potentially contains precious information (as will be discussed in Section 5) and has to be taken into account when testing it (as will be discussed in Section 6), can be quantified by introducing in the modelization a further parameter commonly called "sample variance" or "slop". The issue of fitting data with a power-law by accounting simultaneously for X and Y errors and for sample variance has been faced e.g. by Reichart et al. (2001) and Reichart & Nysewander (2006) when analyzing the peak luminosity-variability correlation in GRBs.

The methods used in these works are based on a likelihood function derived with a bayesian approach to the prob-

lem; however, recently D'Agostini (2005) and Guidorzi et al. (2006) showed that the correct likelihood function is slightly different from that used by Reichart et al. (2001); Reichart & Nysewander (2006). I applied the method by D'Agostini (2005) and Guidorzi et al. (2006) to the sample of 41 GRBs considered above; with this modelization the parameters are the index and normalization of the power-law ( $m$  and  $K$ ) and the logarithmic dispersion of  $E_{\text{p},i}$  ( $\sigma_{\log E_{\text{p},i}}$ ). The result of this analysis is reported in the last line of Table 3. The values of the index and normalization of the best-fit power-law,  $\sim 0.5$  and  $\sim 100$ , respectively, lie in the ranges of values found with different samples by adopting the simple power-law fit and are coincident with those usually assumed in the literature when comparing new data with the  $E_{\text{p},i} - E_{\text{iso}}$  correlation or using it as an input or required output for GRBs/XRFs synthesis models (see next Section), basing on the early results from Amati et al. (2002) (Table 1, first line). The best fit power-law obtained with this method is plotted in Figures 2 and 3 as a continuous line. The value of the sample variance resulting from the fit is  $\sigma_{\log E_{\text{p},i}} = 0.15^{+0.04}_{-0.04}$  (90% c.l.); in Figures 1 and 2 I show the region,

delimited by two dotted lines, corresponding to deviations of  $E_{\text{p,i}}$  from the best fit power-law of  $\sim 2.5\sigma_{\log E_{\text{p,i}}}$ , assuming  $\sigma_{\log E_{\text{p,i}}} = 0.15$  (the central value of the 90% confidence interval). For a comparison, as shown in Figure 4, the dispersion of the  $\log(E_{\text{p,i}})$  central values around the best fit power-law obtained without accounting for sample variance (line 7 of Table 3) can be fitted with a Gaussian with dispersion  $\sim 0.21$ , consistently with previous analysis based on smaller samples. A similar value ( $\sigma_{\log E_{\text{p,i}}} \sim 0.2$ , is obtained when computing the scatter of the central data points around the law  $E_{\text{p,i}} = 95 \times E_{\text{iso}}^{0.49}$ ). This value is of course higher than sample variance, because it includes statistical fluctuations; if one considers this as the overall dispersion of the correlation, then the two dotted lines in Figures 2 and 3 delimitate the  $\pm 2\sigma$  region. An estimate of the sample variance characterizing the  $E_{\text{p,i}} - E_{\text{iso}}$  correlation was also performed by Lamb, Donaghy & Graziani (2005), who, based on a smaller sample and following a different method, derived a value of  $\sim 0.13$ .

Finally, from Figure 3, it can be seen that the uncertain values and upper/lower limits of  $E_{\text{p,i}}$  and  $E_{\text{iso}}$  of classical long GRBs and XRFs (reported in Table 2) are consistent with the  $E_{\text{p,i}} - E_{\text{iso}}$  correlation, including *Swift* GRBs. Figure 3 also shows clearly that the  $E_{\text{p,i}} - E_{\text{iso}}$  plane can be very useful in discriminating different classes of GRBs. Indeed, both sub-energetic GRBs (GRB980425 and, possibly, GRB031203) and short GRBs (050709 and 051221) are clear outliers of the correlations, showing  $E_{\text{iso}}$  values too low with respect to their peak energies, which range within those of normal GRBs (Figure 1, right panel).

During the reviewing process of this article, firm estimates of both  $z$  and  $E_{\text{p,obs}}$  have become available for 4 more *Swift* events (GRB060115, GRB060124, GRB060206, GRB060418), based on spectral measurements from *Swift*, HETE-2, Konus. The  $E_{\text{p,i}}$  and  $E_{\text{iso}}$  of these events are all fully consistent with the  $E_{\text{p,i}} - E_{\text{iso}}$  correlation.

## 5 MAIN IMPLICATIONS AND DISCUSSION

The analysis presented in previous Sections, based on an updated sample containing about twice events with respect to previous works and including the recent *Swift* GRBs, confirms and strengthens the  $E_{\text{p,i}} - E_{\text{iso}}$  correlation for long GRBs/XRFs and gives its best characterization up to now in terms of index and normalization of the best-fit power-law and of its dispersion. Remarkably, the correlation now extends over  $\sim 5$  orders of magnitude in  $E_{\text{iso}}$ ,  $\sim 3$  orders of magnitude in  $E_{\text{p,i}}$  and over a redshift range  $\sim 0.15 < z < 4.5$  (but also the highest  $z$  event, GRB050904 at  $z=6.29$ , has  $E_{\text{p,i}}$  and  $E_{\text{iso}}$  values consistent with it). Since its discovery in 2002 (Amati et al. 2002) and in particular its confirmation and extension to XRFs (Amati 2003; Lamb, Donaghy & Graziani 2004; Sakamoto et al. 2004), the origin of the  $E_{\text{p,i}} - E_{\text{iso}}$  correlation and its implications for GRB models have been investigated by several works. The impact of this robust observational evidence on prompt emission models concerns mainly the physics, the geometry (i.e. shape and properties of jets), viewing angle effects and GRB/XRF unification. Indeed, the existence of the  $E_{\text{p,i}} - E_{\text{iso}}$  correlation and its properties are also often used as an ingredient or a test

output for GRB synthesis models, as in the case of, e.g., the GRB/XRF model by Barraud et al. (2005), the multi-subjets model by Toma, Yamazaki & Nakamura (2005), the uniform jet model by Lamb, Donaghy & Graziani (2005), the study of the impact of off-jet relativistic kinematics by Donaghy (2006), the dissipative photosphere models by Rees & Mešzařos (2005), the supercritical pile model by Mastichiadis & Kazanas (2006). Another important outcome of the analysis presented in this paper is the clear evidence that, in addition to the peculiar sub-energetic GRB980425 (and possibly GRB031203), short GRBs do not follow the  $E_{\text{p,i}} - E_{\text{iso}}$  correlation, as suggested by the different location between long and short BATSE GRBs in the hardness-intensity plane. Below I summarize these topics and discuss also the possible origin of the extra-Poissonian dispersion of the correlation.

### 5.1 Physics of prompt emission

The physics of the prompt emission of GRBs is still far to be settled and a variety of scenarios, within the standard fireball picture, have been proposed, based on different emission mechanisms (e.g. SSM internal shocks, Inverse Compton dominated internal shocks, SSM external shocks, photospheric emission dominated models) and different kinds of fireball (e.g. kinetic energy dominated or Poynting flux dominated), see e.g. Zhang & Mészáros (2002) for a review. In general, both  $E_{\text{p,i}}$  and  $E_{\text{iso}}$  are linked to the fireball bulk Lorentz factor,  $\Gamma$ , in a way that varies in each scenario, and the existence and properties of the  $E_{\text{p,i}} - E_{\text{iso}}$  correlation allow to constrain the range of values of the parameters, see, e.g., Zhang & Mészáros (2002) and Schaefer (2003). For instance, as shown, e.g., by Zhang & Mészáros (2002), Ryde (2005) and Rees & Mešzařos (2005), for a power-law electron distribution generated in an internal shock within a fireball with bulk Lorentz factor  $\Gamma$ , it is possible to derive the relation  $E_{\text{p,i}} \propto \Gamma^{-2} L^{1/2} t_{\nu}^{-1}$ , where  $L$  is the GRB luminosity and  $t_{\nu}$  is the typical variability time scale. Clearly, in order to produce the observed  $E_{\text{p,i}} - E_{\text{iso}}$  correlation the above formula would require that  $\Gamma$  and  $t_{\nu}$  are approximately the same for all GRBs, an assumption which is difficult to justify. Things get even more complicated if one takes into account that the models generally assume  $L \propto \Gamma^{\beta}$ , with the value of  $\beta$  varying in each scenario and is typically  $\sim 2-3$  (Zhang & Mészáros 2002; Schaefer 2003; Ramirez-Ruiz 2005; Ryde 2005). More specific examples of the constraints put by the  $E_{\text{p,i}} - E_{\text{iso}}$  correlation on the parameters of SSM and IC based emission models, both in internal and external shocks, can be found, e.g., in Zhang & Mészáros (2002); Schaefer (2003). An interesting possibility, which is currently the subject of many theoretical works, is that a substantial contribution to prompt radiation of GRBs comes from direct or Comptonized thermal emission from the photosphere of the fireball (Zhang & Mészáros 2002; Ryde 2005; Rees & Mešzařos 2005; Ramirez-Ruiz 2005). This could explain the very hard spectra observed at the beginning of several events (Preece et al. 2000; Frontera et al. 2000b; Ghirlanda, Celotti & Ghisellini 2003), inconsistent with SSM models, and the smooth curvature characterizing GRBs average spectra. In this scenarios,  $E_{\text{p,i}}$  is mainly determined by the peak temperature  $T_{pk}$  of black-body distributed photons and thus naturally linked to the lumi-

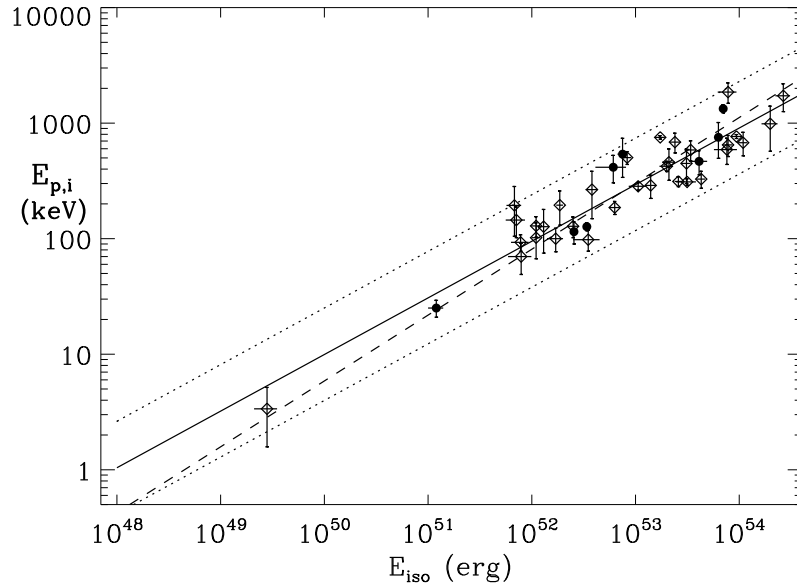


**Figure 2.**  $E_{p,i}$  and  $E_{\text{iso}}$  values for 41 GRBs/XRFs with firm redshift and  $E_{p,\text{obs}}$  estimates. Filled circles correspond to *Swift* GRBs. The continuous line is the best fit power-law  $E_{p,i} = 95 \times E_{\text{iso}}^{0.49}$  obtained by accounting for sample variance; the dotted lines delimit the region corresponding to a vertical logarithmic deviation of 0.4. The dashed line is the best fit power-law  $E_{p,i} = 77 \times E_{\text{iso}}^{0.57}$  obtained by fitting the data without accounting for sample variance. See text for details.

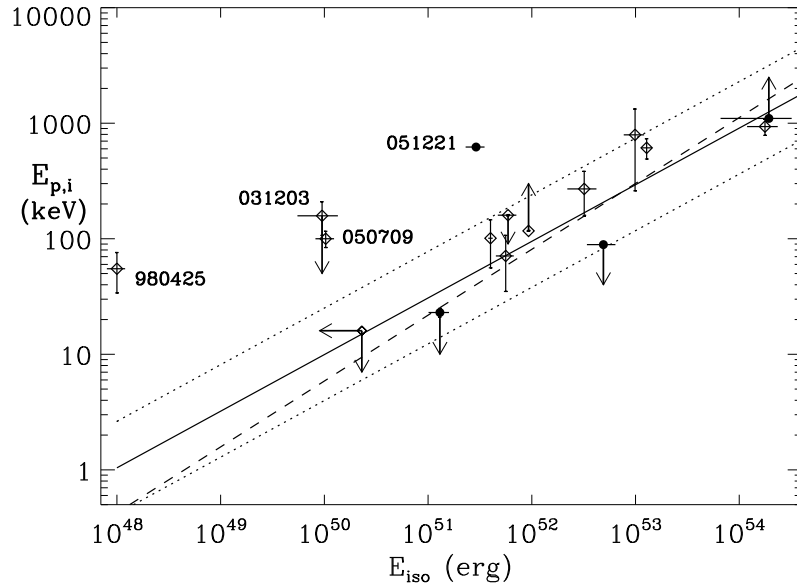


**Figure 3.** Same as Figure 2 for the 12 GRBs with uncertain estimates of  $z$  and/or  $E_{p,\text{obs}}$ , for the peculiar sub-energetic event GRB980425 / SN1998bw and for the two short GRBs 050709 and 051221.

nosity or radiated energy. For instance, for Comptonized emission from the photosphere one can derive the relations  $E_{p,i} \propto \Gamma T_{pk} \propto \Gamma^2 L^{-1/4}$  or  $E_{p,i} \propto \Gamma T_{pk} \propto r_0^{-1/2} L^{1/4}$  (where  $r_0$  is a particular distance between the central engine and the emitting region), depending on the assumptions made (Rees & Meščářos 2005). Also in this case, off course, the  $L \propto \Gamma^\beta$  relation plays a decisive role. As shown

by Rees & Meščářos (2005), in this scenario the correct  $E_{p,i}$  –  $E_{\text{iso}}$  relation can be obtained for some specific physical conditions just below the photosphere.

Finally, also, the fact that the  $E_{p,i}$  distribution is broader than inferred previously basing mainly on the observed  $E_{p,\text{obs}}$  values of bright BATSE GRBs, as shown in

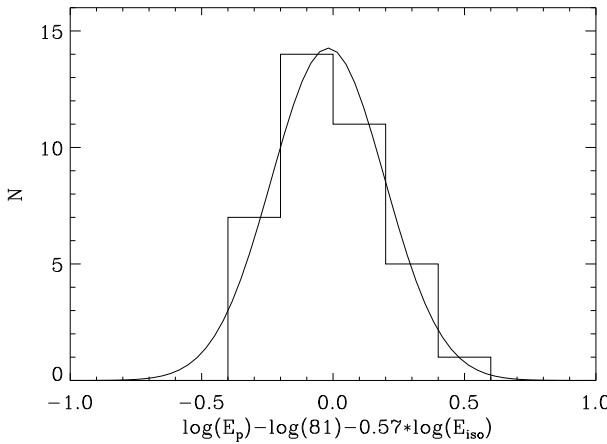


**Figure 4.** Logarithmic dispersion of the  $E_{p,i}$  values of the 41 GRBs with firm redshift and  $E_{p,i}$  estimates around the power-law best fitting the  $E_{p,i} - E_{\text{iso}}$  correlation without accounting for sample variance. I also show the best fit Gaussian, which has a dispersion of  $\sigma_{\log(E_{p,i})} \sim 0.21$ .

Figure 1, can put important constraints on models for the physics of GRB prompt emission (Zhang & Mészáros 2002).

## 5.2 Jets, viewing angle effects and GRB/XRF unification models

The validity of the  $E_{p,i} - E_{\text{iso}}$  correlation from the most energetic GRBs to XRFs (see Figure 2) confirms that these two phenomena have the same origin and is a very challenging observable for GRB jet models. Indeed, these models have to explain not only how  $E_{\text{iso}}$  and  $E_{p,i}$  are linked to the jet opening angle,  $\theta_{jet}$ , and/or to the viewing angle with respect to the jet axis,  $\theta_v$ , but also how  $E_{\text{iso}}$  can span over several orders of magnitudes. In the most simple scenario, the uniform jet model (Frail et al. 2001; Lamb, Donaghy & Graziani 2005), jet opening angles are variable and the observer measures the same value of  $E_{\text{iso}}$  independently of  $\theta_v$ . In the other popular scenario, the universal structured jet model (e.g. Rossi, Lazzati & Rees ),  $E_{\text{iso}}$  depends on  $\theta_v$ . As discussed in Section 2, in the hypothesis that achromatic breaks found in the afterglow light curves of some GRBs with known redshift are due to collimated emission, it was originally found (Frail et al. 2001; Berger, Kulkarni & Frail 2003) that the collimation corrected radiated energy,  $E_\gamma$ , is of the same order ( $\sim 10^{51}$  erg) for most GRBs and that  $E_{\text{iso}} \propto \theta_{jet}^{-2}$ , assuming a uniform jet. In the case of structured jet models, which assume that  $\theta_{jet}$  is similar for all GRBs (hence this scenario is also called universal jet model) the same observations imply that  $E_{\text{iso}} \propto \theta_v^{-2}$ . Thus, always under the assumption of a nearly constant  $E_\gamma$ , the found  $E_{p,i} - E_{\text{iso}}$  correlation implies  $E_{p,i} \propto \theta_{jet}^{-1}$  and  $E_{p,i} \propto \theta_v^{-1}$  for the uniform and structured jet models, respectively. Lamb, Donaghy & Graziani (2005) argue that the structured universal jet model, in order to explain the validity of the  $E_{p,i} - E_{\text{iso}}$  correlation from XRFs to energetic GRBs, predicts a number of detected XRFs several orders of magnitude higher than the observed one ( $\sim 1/3$  than that of GRBs). In their view, the uniform jet model

can overcome these problems by assuming a distribution of jet opening angles  $N(\theta_{jet}) \propto \theta_{jet}^{-2}$ . This implies that the great majority of GRBs have opening angles smaller than  $\sim 1^\circ$  and that the true rate of GRBs is several orders of magnitude higher than observed and comparable to that of SN Ic. On the other hand, Zhang et al. (2004) show that the requirement that most GRBs have jet opening angles less than 1 degree, needed in the uniform jet scenario in order to explain the  $E_{p,i} - E_{\text{iso}}$  correlation, as discussed above, implies values of the fireball kinetic energy and/or of the interstellar medium density much higher than those inferred from the afterglow decay light curves. Together with other authors, e.g. Lloyd-Ronning, Dai & Zhang (2004); Dai & Zhang (2005), they propose a modification of the universal structured jet model, the quasi-universal Gaussian structured jet. In this model, the measured  $E_{\text{iso}}$  undergoes a mild variation for values of  $\theta_v$  inside a typical angle, which has a quasi-universal value for all GRBs/XRFs, whereas it decreases very rapidly (e.g. exponentially) for values outside the typical angle. In this way, the universal structured jet scenario can reproduce the  $E_{p,i} - E_{\text{iso}}$  correlation and predict the observed ratio between the number of XRFs and that of GRBs. Recently, a Fisher-shape has been proposed, for both the variable angle and universal angle scenarios (Donaghy, Graziani & Lamb 2005; Dai & Zhang 2005), as a very promising alternative, in particular for the explanation of the validity of the  $E_{p,i} - E_{\text{iso}}$  correlation from the brightest GRBs to XRFs. Other jet models proposed very recently that can reproduce the  $E_{p,i} - E_{\text{iso}}$  correlation include the ring-shaped jet model, see Eichler & Levinson (2004), and the multi-component (sub-jets) model, see Toma, Yamazaki & Nakamura (2005).

Of particular interest are the off-axis scenarios, in which the jet is typically assumed to be uniform but, due to relativistic beaming and Doppler effects, for  $\theta_v > \theta_{jet}$  the measured emissivity does not sharply go to zero and the event is detected by the observer with  $E_{\text{iso}}$  and  $E_{p,i}$  dropping rapidly as  $\theta_v$  increases (Yamazaki, Ioka & Nakamura 2003; Granot et al. 2002; Eichler & Levinson 2004; Donaghy 2006). In these models, XRFs are those events seen very off-axis and the XRFs rate with respect to GRBs and the  $E_{p,i} - E_{\text{iso}}$  correlation can be correctly predicted. As shown e.g. in Yamazaki, Ioka & Nakamura (2004) for a simple model of GRB jet, if the Doppler shift factor is  $\delta = [\Gamma(1 - \beta \cos(\theta_v - \theta_{jet}))]^{-1}$  (where  $\beta$  is the velocity of the outflow in units of speed of light),  $E_{p,i}$  and  $E_{\text{iso}}$  scale, with respect to their values observable at the edge of the jet, as  $E_{p,i} \propto \delta$  and  $E_{\text{iso}} \propto \delta^{1-\alpha}$ , where  $\alpha$  is the spectral index of the prompt emission photon spectrum in the hard X-ray energy band. By combining these relations one can obtain the  $E_{p,i} - E_{\text{iso}}$  correlation with index 0.5 for classical GRBs ( $\alpha \sim -1$ ) and 0.3 for XRFs ( $\alpha \sim -2$ ). A detailed study of off-jet relativistic kinematics effects has been recently performed by Donaghy (2006) for a set uniform (i.e. top hat shaped – variable opening angle) jet models, finding that these scenarios predict a significant population of bursts away from the  $E_{p,i} - E_{\text{iso}}$  correlation, unless  $\Gamma > 300$  for all bursts or there is a strong anti-correlation between  $\Gamma$  and the jet solid angle. Finally, the off-axis effects for very weak and soft events can be applied in a similar way as described above in the context of the cannon ball (CB) model for GRBs in order to reproduce the  $E_{p,i} - E_{\text{iso}}$  correlation (Dar & De Rujula 2004).

### 5.3 The dispersion of the correlation

In addition to its existence and slope, also the extra-Poissonian dispersion of the  $E_{\text{p},i} - E_{\text{iso}}$  correlation is an important source of information. As discussed in Section 3 and shown in Table 3, while the correlation is very highly significant, the scatter of the data around the best fit power-law exceed that expected by statistical fluctuations alone and produces high values of  $\chi^2_{\nu}$ . By fitting with a Gaussian the dispersion of the central values of  $\log(E_{\text{p},i})$  around the best fit model, I obtain  $\sigma_{\log E_{\text{p},i}} \sim 0.2$ , while by fitting the whole data with the method by D'Agostini (2005), which includes sample variance directly in the model, I obtain  $\sigma_{\log E_{\text{p},i}} = 0.15^{+0.4}_{-0.4}$ . A similar scatter, even if computed with only the first of the two methods reported above, is found for the  $E_{\text{p},i} - L_{\text{iso}}$  and  $E_{\text{p},i} - L_{\text{peak,iso}}$  correlations, see, e.g., Ghirlanda et al. (2005a). Intriguingly, the  $E_{\text{p},i} - E_{\gamma}$  correlation shows instead a lower dispersion, of the order of  $\sigma_{\log E_{\text{p},i}} \sim 0.1$  (Ghirlanda, Ghisellini & Lazzati 2004; Nava et al. 2006), even if this correlation is based on a still low number of events, it requires an estimate of  $t_b$  in addition to  $E_{\text{p},\text{obs}}$  and  $z$ , it depends on jet model and circum-burst environment properties (density, distribution) and there are possible outliers, as discussed e.g. by Friedman & Bloom (2005) and may be indicated by the lack of break in the X-ray afterglow light curve of some *Swift* GRBs with known redshift. A low 3-D dispersion characterizes also the  $E_{\text{p},i} - E_{\text{iso}} - t_b$  correlation, which is a kind of model-independent version of the  $E_{\text{p},i} - E_{\gamma}$  correlation (Liang & Zhang 2005; Nava et al. 2006). The existence of both the  $E_{\text{p},i} - E_{\text{iso}}$  and  $E_{\text{p},i} - E_{\gamma}$  correlations is due to the fact that the collimation angles of GRBs are distributed over a relatively narrow range of values; the lower dispersion of the  $E_{\text{p},i} - E_{\gamma}$  correlation indicates that at least part of the scatter of the  $E_{\text{p},i} - E_{\text{iso}}$  correlation is due to the dispersion of jet opening angles. And indeed, the comparison of the properties of the two correlations has been used, in addition to the study of the relation between jet opening angle and radiated energy, to infer the distribution of jet opening angles, as done, e.g., by Ghirlanda, Ghisellini & Firmani (2005); Bosnjak et al. (2006a); Donaghy (2006). Very recently, it has been found evidence that a relevant contribution to the dispersion of the correlation is due to temporal properties of the prompt emission, like the half-width of the auto-correlation function (Borgonovo & Bjornsson 2006) and the "high-signal" time scale (Firmani et al. 2006). Other contribution to the scatter of the  $E_{\text{p},i} - E_{\text{iso}}$  correlation may come from viewing angle effects, e.g. Levinson & Eichler (2005), the dispersion of the parameters of the fireball and/or of the time scales (as discussed in Section 5.1 concerning synchrotron emission in internal shocks), the inhomogeneous structure of the jet, e.g. Toma, Yamazaki & Nakamura (2005), the possible presence of significant amount of material in the circum-burst region, that would affect the estimates of both  $E_{\text{iso}}$  and  $E_{\text{p},i}$  with a global qualitative effect of steepening the correlation and increasing its dispersion (Longo et al. 2005). In general, several GRB population synthesis models, like those mentioned at the beginning of this Section, predict a scatter of the  $E_{\text{p},i} - E_{\text{iso}}$  correlation which depend on the parameters values.

When investigating the above physical interpretations and implications, it is important to take into account that

at least part of the dispersion of the  $E_{\text{p},i} - E_{\text{iso}}$  correlation could arise from instrumental and other systematic effects in the estimates of  $E_{\text{p},i}$  and  $E_{\text{iso}}$  and their uncertainties. As discussed e.g. by Lloyd, Petrosian & Mallozzi (2000); Lloyd & Petrosian (2002), data truncation effects, i.e. the systematics introduced by the limited energy band of the detector, may affect significantly the estimate of  $E_{\text{p},\text{obs}}$ . Indeed, as discussed in Section 2, typical GRB spectra are characterized by a very smooth curvature and cover  $\sim 3$  orders of magnitude or more in photon energy. Thus, unless the energy band extends from few keV to few MeV, only a portion of the spectrum can be detected by a single instrument, which may cause a bias in the estimate of the spectral parameters, especially when  $E_{\text{p},\text{obs}}$  is not far from the low or high thresholds. Also, both *BeppoSAX* ( $\sim 2$ –700 keV) and HETE-2 (2–400 keV), in addition to be capable to detect X-ray rich events and XRFs which could not be triggered by BATSE ( $\sim 25$ –2000 keV), showed that X-ray emission below  $\sim 30$  keV of normal GRBs can last up to several tens of seconds more than in the hard X-ray energy band. Thus, a GRB detector working at energies higher than few tens of keV, like BATSE, may have lost, for a fraction of GRBs, a substantial portion of the soft X-ray emission, with a consequent overestimate of  $\alpha$  and  $E_{\text{p},\text{obs}}$ . These effects can indeed be seen when comparing the X- and hard X-rays duration and light curves of *BeppoSAX* (Frontera et al. 2000b; Amati et al. 2002) and HETE-2 (Sakamoto et al. 2005b) GRBs and the average spectral parameters estimated by *BeppoSAX* /WFC+GRBM and BATSE (Amati et al. 2002; Jimenez, Band & Piran 2001) for those events revealed by both satellites. This is true, even if to a minor extent, when comparing the best fit spectral models obtained with HETE-2/FREGATE (7–400 keV) alone (Barraud et al. 2003) with those obtained by jointly fitting HETE-2/WXM (2–30 keV) and HETE-2/FREGATE data (Sakamoto et al. 2005b).

Concerning  $E_{\text{iso}}$ , the main source of possible systematics is the extrapolation to the 1–10000 keV cosmological rest-frame energy band of the spectral model obtained by fitting data in the instrument energy band (see Section 2). Indeed, the (known) statistical uncertainties and (unknown) biases in the estimates of spectral parameters may affect significantly the estimate of  $E_{\text{iso}}$ . This is particularly true for estimates based on spectra from instruments with high energy bound at a few hundreds of keV, like HETE-2 or *Swift* /BAT, which in several cases cannot provide a reliable estimate of the high energy spectral index  $\beta$ . In addition, the typical choice of computing  $E_{\text{iso}}$  in the 1–10000 keV rest-frame energy band may not be optimal for very soft events with values of  $E_{\text{p},i}$  below a few tens of keV, for which this method can likely lead to an underestimate of  $E_{\text{iso}}$ . Of course, also the choice of the cosmological parameters for the computation of the luminosity distance, usually made by assuming values in the ranges given by the so called "concordance cosmology" based on type Ia SNe and CMB measurements, affects the values of  $E_{\text{iso}}$ .

Finally, very recently *Swift* /XRT found evidence of X-ray flares following the end of the prompt emission as detected by *Swift* /BAT, e.g. Burrows et al. (2005). One possible interpretation of these phenomena is that they are due to continued activity of the engine and/or late internal shocks (Fan & Wei 2005; Burrows et al. 2005; Wu et al.

2006; Perna et al. 2006; Proga & Zhang 2006) and thus can be considered part of the prompt emission. Given that these events are typically soft and that their fluence can be a significant fraction of that of the GRB, their non-detection (because of sensitivity) by past and current GRB detectors may also have biased the estimates of  $E_{\text{iso}}$  (under-estimate) and of  $E_{\text{p},\text{i}}$  (over-estimate).

#### 5.4 Short GRBs

In the past, the  $E_{\text{p},\text{i}} - E_{\text{iso}}$  correlation has been studied basing on data of long GRBs, given that no redshift information was available for short GRBs. Nevertheless, thanks to the measurements performed by HETE-2 and *Swift*, in the last year it has been possible to detect afterglow emission and possible optical counterparts and/or host galaxies for a few short GRBs. As discussed in Section 3, I have included in the analysis reported in this paper the two short GRBs with firm estimates of  $z$  and  $E_{\text{p},\text{obs}}$ : GRB050709 (Villasenor et al. 2005; Hjorth et al. 2005) and GRB051221 (Golenetskii et al. 2005e; Berger & Soderberg 2005). As can be clearly seen in Figure 3, these events are outliers to the  $E_{\text{p},\text{i}} - E_{\text{iso}}$  correlation, even when taking into account its extra-Poissonian dispersion. In addition, the spectral data of other recently localized short GRBs with possible redshifts, GRB050509b (Gehrels et al. 2005; Pedersen et al. 2005), GRB050724 (Krimm et al. 2005; Berger et al. 2005) and GRB050813 (Sato et al. 2005b; Berger 2005), indicate a likely inconsistency with the  $E_{\text{p},\text{i}} - E_{\text{iso}}$  correlation, even though an estimate of  $E_{\text{p},\text{obs}}$  was not possible for these events. These evidences confirm the expectations based on the fact that short GRBs tend to form a separate class with respect to long GRBs in the hardness-intensity plane, i.e. they tend to be weaker and harder, and clearly shows the potentiality of the use of the  $E_{\text{p},\text{i}} - E_{\text{iso}}$  plane for distinguishing different classes of GRBs and understanding their nature. In particular, given that short and long GRBs partially overlap in the hardness-intensity and hardness-duration planes, that a fraction of short GRBs show a softer extended emission which can last tens of seconds, e.g. Norris & Bonnell (2006), the possible relevant impact of spectral/temporal trigger selection effects, it is sometimes difficult to establish to which class a GRB belongs. Thus the  $E_{\text{p},\text{i}} - E_{\text{iso}}$  plane may be a powerful tool under this respect, especially when combined e.g with the lack of spectral lag and spectral evolution which seems to characterize short GRBs (Norris & Bonnell 2006).

While the commonly accepted hypothesis for the progenitors of long GRBs is their association with the core collapse of massive fastly rotating stars (so called "hypernova" or "collapsar" models), based on their duration (from few seconds up to hundreds of seconds), their huge  $E_{\text{iso}}$  (Figure 1), their typical location inside blue galaxies with high star formation rate and the evidence of a metal-rich circum-burst environment (as inferred from absorption / emission features in prompt and afterglow emission spectra), short GRBs are thought to originate from the coalescence of neutron star – neutron star or neutron star – black hole binaries (the "merger" scenarios). It has also been proposed that a fraction of them may be giant flare from extra-galactic soft gamma repeaters, see, e.g., Mészáros (2002); Piran (2005) for reviews. The very recent observations mentioned above,

show that, as long GRBs, also short GRBs lie at cosmological distances ( $0.1 < z < 1$ ) but they are less energetic (see Table 1 and Figures 1 and 3). Also, their host galaxies show different morphologies and star forming activity: for instance, short GRB050724 (as possibly short GRB050509b) came from an elliptical galaxy with low star formation, whereas short GRB050709 was associated with an irregular late type star forming galaxy. Both events were located towards the outskirts of their host galaxies. All these properties match the predictions of the merger scenarios (e.g. Belczynski et al. 2006). Off course, these evidences concern still a very low number of short GRBs and thus it is premature to draw any definitive conclusion. Anyway, the different nature of the progenitors between short and long GRBs can help in understanding their different behavior in the  $E_{\text{p},\text{i}} - E_{\text{iso}}$  plane. Ghirlanda, Ghisellini & Celotti (2004) found, basing on BATSE data, that the emission properties of short GRBs are similar to those of the first  $\sim 1\text{--}2$  s of long GRBs. This could indicate that the central engine is the same for the two classes, but works for a longer time in long GRBs. This would explain the low radiated energy by short GRBs and, given that the emission would stop before the typical hard to soft evolution observed for long GRBs, also their high  $E_{\text{p},\text{i}}$  (with respect to their  $E_{\text{iso}}$ ). The merger scenarios naturally explain the short life of the central engine, and thus the low radiated energy and the quitting of the emission before hard to soft spectral evolution. In addition, they also predict a weak afterglow emission, as recently observed (Fox et al. 2005), because of the cleaner and lower density circum-burst medium with respect to that predicted by the hypernova scenarios for long GRBs, which would cause a very inefficient external shock. In the GRB scenarios where most of the prompt emission of long GRBs is due to the external shock too, this naturally explains the lack of long lasting and softening emission in short GRBs. Again, this would produce an high average  $E_{\text{p},\text{i}}$  value with respect to the radiate energy, and thus the inconsistency with the  $E_{\text{p},\text{i}} - E_{\text{iso}}$  correlation holding for long GRBs. Finally, in order to explain the very low or 0 spectral lag observed in short GRBs with respect to long GRBs, Norris & Bonnell (2006) consider the hypothesis that the typical  $\Gamma$  of short events is several times that of long ones, and thus of the order of  $\sim 500\text{--}1000$ , as predicted e.g by the merger model of Aloy, Janka & Muller (2005). With such a high Lorentz factor, internal shocks are expected to have a low efficiency, and indeed this is one possible explanation for the weakness and softness of XRFs (e.g Barraud et al. 2005). If we assume the scenario proposed by e.g. Ghirlanda, Celotti & Ghisellini (2003), in which the spectrally hard emission observed in the first seconds of long GRBs is due to (possibly Compton dragged) thermal emission from the photosphere and the later emission to synchrotron processes occurring in internal shocks, the high  $\Gamma$  would thus produce a short-hard emission possibly followed by a weak soft component, as observed for several short GRBs (Villasenor et al. 2005; Norris & Bonnell 2006).

#### 5.5 Sub-energetic GRBs and the GRB/SN connection

As can be seen in Figure 3, in addition to the two short GRBs also the prototype event for the GRB/SN connection, GRB980425/SN1998bw, is characterized by values of

$E_{p,i}$  and  $E_{iso}$  completely inconsistent with the  $E_{p,i} - E_{iso}$  correlation holding for the other events. From an observational point of view, this is a direct consequence of the fact that the event is characterized by a fluence and a measured peak energy in the range of classical long GRBs but, based on the commonly accepted association with SN1998bw, it lies at a much lower distance ( $z = 0.0085$ ). Figure 3 shows that also another event associated with a SN event, GRB031203, is characterized by a value of  $E_{p,i}$  which, combined with its low value of  $E_{iso}$ , makes it completely inconsistent with the correlation. Given that GRB031203 is the most similar event to GRB980425 under several points of view (although lying at a larger distance,  $z \sim 0.1$ ), in particular the strong evidence of association with a SN event (SN2003lw) and the low afterglow energy inferred from radio observations (Soderberg et al. 2004; Sazonov, Lutovinov & Sunyaev 2004), this inconsistency has been invoked as a further evidence of the existence of a class of close sub-energetic GRBs. However, the lower limit on  $E_{p,i}$  based on ISGRI data (Sazonov, Lutovinov & Sunyaev 2004) and the  $E_{p,i}$  estimate based on Konus data (Table 2, Ulanov et al. 2005) are currently debated based on the dust echo observed with XMM-Newton, which could indicate a much softer prompt emission spectrum (Watson et al. 2006). The sample of GRBs with most evidence of association with a SN include also GRB030329 (SN2003dh) and GRB021211 (SN2002lt), which, in converse, are not sub-energetic and are characterized by  $E_{p,i}$  and  $E_{iso}$  values fully consistent with the  $E_{p,i} - E_{iso}$  correlation. The fact the two closest and sub-energetic among those GRBs most clearly associated with a SN are outliers to the  $E_{p,i} - E_{iso}$  correlation is intriguing. As in the case of short GRBs, these evidences show the potential use of the  $E_{p,i} - E_{iso}$  plane to distinguish among different sub-classes of GRBs, and have important implications for GRB/XRF/SN unification models. The most common explanations assume that the peculiarity of these events is due to particular and uncommon viewing angles, as proposed e.g. by Yamazaki, Yonetoku & Nakamura (2003) for GRB980425 and Ramirez-Ruiz et al. (2005) for GRB031203. Based on relativistic beaming and Doppler effects and the assumption of a uniform jet, they find that  $E_{p,i} \propto \delta$  and  $E_{iso} \propto \delta^3$ , where  $\delta$  is the relativistic Doppler factor (see Section 5.2). For large off-axis viewing angles the different dependence of  $E_{p,i}$  and  $E_{iso}$  on  $\delta$  would cause significant deviations from the  $E_{p,i} - E_{iso}$  correlation. An alternative explanation has been suggested by Dado & Da3 (2005) in the framework of the CB model (Dar & De Rujula 2004). In this scenario, the  $\nu F_\nu$  spectra of GRBs are characterized by two peaks, one at sub-MeV energies, the normal peak following the  $E_{p,i} - E_{iso}$  correlation, and one in the GeV-TeV range. When a GRB is seen very off-axis, the same relativistic Doppler and beaming effects discussed above would shift the high energy peak at low energies, making it to be confused with the normal low energy GRB peak. Very recently, off-axis scenarios have been seriously challenged by the detection of a very close ( $z = 0.0331$ ) and sub-energetic event, GRB060218/SN2006aj, which, contrary to GRB980425, is characterized by  $E_{p,i}$  and  $E_{iso}$  values fully consistent with the  $E_{p,i} - E_{iso}$  correlation (Amati et al. 2006; Ghisellini et al. 2006).

Finally, Bosnjak et al. (2006b), based on BATSE data of

GRBs with unknown redshift found evidence that a part of GRB with indications of association with a SN are inconsistent with the  $E_{p,i} - E_{iso}$  correlation, as also the lag-luminosity relation (Norris, Marani & Bonnell 2000), for any value of  $z$ , which would confirm the existence of a peculiar class of sub-energetic, SN-associated events. See, however, next Section for a discussion of this method.

## 6 THE $E_{p,i} - E_{iso}$ CORRELATION AND GRBS WITH UNKNOWN REDSHIFT

### 6.1 Pseudo-redshifts, GRB luminosity function, cosmology

The existence of correlations between intrinsic properties of GRBs, emerged in the last years thanks to the increasing number of GRBs with known redshift, has stimulated their use for the estimate of pseudo-redshifts for large samples of BATSE GRBs. In turn, the pseudo-redshifts estimates have been used to compute the luminosity of large samples of GRBs and infer their luminosity function. This has been done mainly with the correlation between spectral lag and luminosity discovered by Norris, Marani & Bonnell (2000), the variability – peak luminosity correlation (Reichart et al. 2001; Reichart & Nysewander 2006; Guidorzi et al. 2005), and the  $E_{p,i} - \text{peak luminosity}$  correlation (Yonetoku et al. 2004). In addition, the  $E_{p,i} - E_\gamma$  and  $E_{p,i} - E_{iso} - t_b$  correlations, given their low dispersion, have been used for the estimate of cosmological parameters, e.g., Ghirlanda et al. (2004); Dai, Liang & Xu (2004); Liang & Zhang (2005); Xu, Dai & Liang (2005), in a way similar to that used with type Ia SNe. With respect to all the above correlations, the  $E_{p,i} - E_{iso}$  correlation is based on a much larger sample of GRBs, as shown in this work, and is very highly significant. Also, differently from the  $E_{p,i} - E_\gamma$  and  $E_{p,i} - E_{iso} - t_b$  correlation, which show a lower dispersion but an higher number of possible outliers (as discussed above), the  $E_{p,i} - E_{iso}$  correlation does not require the detection of a break in the afterglow light curve nor a modelization of the GRB jet and circum-burst environment (as needed for the  $E_{p,i} - E_\gamma$  correlation). Thus, in principle the  $E_{p,i} - E_{iso}$  can provide the most reliable pseudo-redshift estimates. The most straightforward method is to take the fluence and spectral parameters of a GRB and compute  $E_{p,i}$  and  $E_{iso}$ , following the same methods used by Amati et al. (2002) or Ghirlanda, Ghisellini & Lazzati (2004), for a grid of  $z$  values (say from 0.01 to 50). The pseudo-redshift range will then be given by the values of  $z$  for which, accounting for the uncertainties on  $E_{p,i}$  and  $E_{iso}$  and for the extra-Poissonian dispersion of the correlation (as quantified in Section 4 and discussed above), the corresponding  $(E_{p,i}, E_{iso})$  points are consistent with the  $E_{p,i} - E_{iso}$  correlation at a given level of significance. In practice, if  $K$  and  $m$  are the normalization and index of the power-law best fitting the  $E_{p,i} - E_{iso}$  correlation ( $\sim 100$  and  $\sim 0.5$  if we assume the values determined in Section 4 by accounting for sample variance),  $E_{p,i}$  and  $E_{iso}$  are the intrinsic peak energy and the isotropic radiated energy at the redshift  $z$ , the significance of the deviation of the  $(E_{p,i}, E_{iso})$  point from the correlation is given by  $\Delta / \sqrt{\sigma_\Delta^2 + \sigma_{corr}^2}$ , where  $\Delta = \log(E_{p,i}) - \log(K) - m \times \log(E_{iso})$ ,  $\sigma_\Delta$  is the uncertainty

on  $\Delta$  computed from  $\sigma_{\log E_{\text{p,i}}}$  and  $\sigma_{\log E_{\text{iso}}}$  by error propagation and  $\sigma_{\text{corr}}$  is the extra-Poissonian dispersion of the correlation (based on the sample variance analysis reported in Section 4, one can for instance assume  $\sigma_{\text{corr}}=0.15$ ). Off course, to be more accurate one should also take into account the uncertainties on  $K$ ,  $m$  and  $\sigma_{\text{corr}}$ ; however,  $K$  and  $m$  are correlated and have low uncertainties (Table 3) and for  $\sigma_{\text{corr}}$  one can conservatively assume the upper bound of the 90% c.l. interval (0.17). This method, as can be seen by testing it on GRBs with known  $z$  and published spectral parameters, like e.g. the *BeppoSAX* events included in the sample of Amati et al. (2002) or the HETE-2 events analyzed by Barraud et al. (2003) and Sakamoto et al. (2005b), provides reliable but often large ranges of pseudo- $z$  (or only lower limits). More precise  $z$  estimates can be obtained with redshift indicators partially based on the  $E_{\text{p,i}} - E_{\text{iso}}$  correlation, like the one developed by Atteia (2003), which provides redshift estimates accurate to a factor of  $\sim 2$  and is currently used to estimate pseudo-redshifts of HETE-2 GRBs, or its refined version proposed very recently by Pelangeon et al. (2006). A caution on the use of these redshift estimators comes from the fact that they are partially empirical and thus are not supported by a complete understanding of the underlying physics.

## 6.2 Tests and selection effects

As already pointed out by Amati et al. (2002), given the relevance of the  $E_{\text{p,i}} - E_{\text{iso}}$  correlation, attention has to be paid to the possible impact of selection effects. Recently, two research groups (Nakar & Piran 2005; Band & Preece 2005), by analyzing BATSE GRBs without known redshift, inferred that  $\sim$ half (Nakar & Piran 2005) or even  $\sim$ 80% (Band & Preece 2005) of the whole GRB population cannot satisfy the correlation for any values of redshift. Thus, they conclude that strong selection effects are introduced in the various steps leading from GRB detection to the final  $z$  estimate and that we are measuring the redshift of only those events that follow the correlation. However, there are increasing evidences that the possible impact of selection effects on the  $E_{\text{p,i}} - E_{\text{iso}}$  correlation and the possible number of outliers are much lower than argued by these authors. First, their conclusions have been questioned by several other authors (Ghirlanda, Ghisellini & Firmani 2005; Bosnjak et al. 2006a; Pizzichini et al. 2006), who found instead that the  $E_{\text{p,obs}}$  and fluence values of most BATSE GRBs with unknown redshift are fully consistent with the  $E_{\text{p,i}} - E_{\text{iso}}$  correlation. The main source of discrepancy between these two different conclusions lies in accounting or not for the observed dispersion of the correlation and for the uncertainties in the  $E_{\text{p,obs}}$  and fluence values. When accounting for both in the way discussed in previous Section, it can be found that only a very small fraction of BASTE GRBs with unknown redshift may be considered outliers to the  $E_{\text{p,i}} - E_{\text{iso}}$  correlation (Ghirlanda, Ghisellini & Firmani 2005; Pizzichini et al. 2006). It has also to be noticed that some of these authors assumed pseudo-redshifts derived by other correlations, like e.g. the lag-luminosity relation, which are necessarily not the  $z$  values corresponding to the  $(E_{\text{p,i}}, E_{\text{iso}})$  with the minor deviation from the  $E_{\text{p,i}} - E_{\text{iso}}$  relation found with GRBs with known redshift. An important effect that should be taken into account when using

BATSE data to test the correlation is that, as discussed in previous Section, given to the lack of coverage of the X-ray band below  $\sim 25$  keV, BATSE is likely to overestimate the  $E_{\text{p,i}}$  values at least for a fraction of GRBs. And indeed, Ghirlanda, Ghisellini & Firmani (2005), by fitting the  $(E_{\text{p,i}}, E_{\text{iso}})$  points of 442 BATSE GRBs with pseudo-redshifts derived by using the lag-luminosity correlation, find a slope and dispersion consistent with the one obtained with GRBs with known redshift, but a higher normalization, which could indicate a systematic overestimate of  $E_{\text{p,i}}$  by BATSE with respect to *BeppoSAX* and HETE-2. I also note that the possible existence of an  $E_{\text{p,i}} - E_{\text{iso}}$  correlation was suggested by Lloyd, Petrosian & Mallozzi (2000) based on BATSE data of GRBs without known redshift.

Secondly, as a check, I applied the pseudo-redshift estimate method described above to a sample of 46 HETE-2 GRBs with spectral parameters and fluences published by Barraud et al. (2003) and Sakamoto et al. (2005b). I considered only those events with both  $\alpha$  and  $E_{\text{p,obs}}$  constrained; I also discharged the few events in the sample of Sakamoto et al. (2005b) with  $\beta > -2$ . When the reported best fit model is a cut-off power-law, I assumed for  $\beta$  the typical value of  $-2.5$ . For those events contained in both samples, I took the spectral parameters from Sakamoto et al. (2005b), given that it reports results based on data from both WXM and FREGATE, whereas the analysis of Barraud et al. (2003) is based on FREGATE data only. The errors on  $E_{\text{p,i}}$  and  $E_{\text{iso}}$  were derived basing on the errors on spectral parameters and fluences reported in the two references. In the estimate of  $E_{\text{iso}}$  as a function of  $z$  I assumed a standard cosmology with  $\Omega_m = 0.3$ ,  $\Omega_\Lambda = 0.7$  and  $H_0 = 65 \text{ km s}^{-1} \text{ Mpc}^{-1}$ ; for the  $E_{\text{p,i}} - E_{\text{iso}}$  correlation I assumed  $K = 100$ ,  $m = 0.5$  and  $\sigma_{\text{corr}} = 0.15$ . I find that 38 events ( $\sim 83\%$ ) are consistent within  $1\sigma$  with the correlation (i.e. show  $\Delta / \sqrt{\sigma_\Delta^2 + \sigma_{\text{corr}}^2} \leq 1$ ), 5 events ( $\sim 11\%$ ) are consistent within  $2\sigma$  and 2 ( $\sim 4\%$ ) within  $3\sigma$  (with values of 2.1 and 2.7). The only event with a substantial deviation from the  $E_{\text{p,i}} - E_{\text{iso}}$  correlation ( $3.82\sigma$ ) is the short GRB020531. It is also important to note that the pseudo-redshift ranges obtained are fully consistent with the observed  $z$  distribution. These results show that at least most of HETE-2 GRBs with unknown  $z$  are potentially fully consistent with the  $E_{\text{p,i}} - E_{\text{iso}}$  correlation holding for long GRBs and give a further evidence that short GRBs do not follow this correlation. Thus, if there are selection effects in the sample of HETE-2 GRBs with known redshift, on which the  $E_{\text{p,i}} - E_{\text{iso}}$  correlation is partly based, they are more likely due to detectors sensitivity as a function of energy than to the subsequent processes leading to redshift estimate. However, the fact that the distribution of these GRBs in the fluence- $E_{\text{p,obs}}$  plane is consistent with that of BATSE events (Figure 16 of Sakamoto et al. 2005b) indicates that the possible inconsistency of a fraction of BATSE GRBs with unknown redshift with the  $E_{\text{p,i}} - E_{\text{iso}}$  correlation may be due to an overestimate of  $E_{\text{p,obs}}$ , as a consequence of the effects discussed above and in Section 5.3.

A third important issue concerns the fact that, as discussed in Section 4 and shown in Figures 2 and 3, all *Swift* GRBs with known redshift are consistent with the  $E_{\text{p,i}} - E_{\text{iso}}$  correlation. This is a strong evidence against the existence of relevant selection effects in the updated sample of GRBs with known redshift on which the  $E_{\text{p,i}} - E_{\text{iso}}$  correlation study

here presented is based, because: a) the burst detection sensitivity of *Swift* /BAT in  $\sim$ 15–300 keV is comparable to that of BATSE and better than that of *BeppoSAX* and HETE–2 (see however Band 2003 for a comparison of the sensitivities of these different detectors as a function of energy), which in the past years contributed nearly all the measurements on which the  $E_{p,i} - E_{iso}$  correlation was based; b) the very fast and precise localization capabilities of *Swift* /XRT allowed to substantially reduce the selection effects also in the process leading to redshift estimate (GRB precise localization, optical follow–up, optical afterglow and/or host galaxy detection and spectroscopy). A drawback of BAT is that it can provide an estimate of  $E_{p,obs}$  only for a small fraction of events (15–20% at most).

Basing on the above, it is unlikely that the  $E_{p,i} - E_{iso}$  correlation is strongly affected by selection effects. Anyway, the existence of sub–classes of GRBs not following it cannot be excluded. As discussed in previous Section, the analysis of the sample of GRBs with known redshift and  $E_{p,obs}$  shows that, in addition to short GRBs, a class of sub–energetic events (like GRB980425 and possibly GRB031203) with spectral–energy properties inconsistent with the correlation may exist. The possible existence of a fraction of long GRBs is also predicted by some GRB synthesis models, like, e.g., the one by Donaghy (2006) based on off–jet relativistic kinematics effects. Obviously, the most reliable test of the  $E_{p,i} - E_{iso}$  correlation and of the existence of one or more sub–classes of outliers will come from the ongoing quick enlargement of the sample of GRBs with known redshift and  $E_{p,obs}$  both in number, thanks to *Swift* fast and precise localizations, and in the coverage of the  $E_{p,obs}$ –fluence plane, as allowed by the GRB experiments with different energy bands and sensitivity presently operating, like *Swift* /BAT, HETE–2, Konus/Wind, Suzaku/WAM, INTEGRAL/ISGRI, or that will fly in the next future, like, e.g., those on board AGILE and GLAST.

## ACKNOWLEDGMENTS

I am grateful to C. Guidorzi and R. Landi for their help in parts of the analysis here reported. I thank F. Frontera, C. Guidorzi and E. Montanari for useful discussions and their contribution to the development of the method used to fit the data accounting for sample variance. I wish also to thank G. Ghirlanda for useful discussion and the anonymous Referee for his/her very careful reading of the paper and for comments and suggestions which improved its quality.

## REFERENCES

Aloy M.A., Janka H.T., Muller E., 2005, *A&A*, 436, 273  
 Amati L. et al., 2002, *A&A*, 390, 81  
 Amati L., 2003, *ChJAA*, 3 Suppl., 455  
 Amati L. et al., 2003, *AIP Proc.*, 662, 387  
 Amati L. et al., 2006, *A&A*, preprint (astro–ph/0607148)  
 Atteia J.-L. , 2003, *A&A*, 407, L1  
 Atteia J.-L. et al., 2005, *ApJ*, 626, 292  
 Band D., Matteson J., Ford L. et al., 1993, 413, 281  
 Band D., 2003, *ApJ*, 588, 945  
 Band D., Preece R., 2005 *ApJ*, 627, 319  
 Barraud C. et al., 2003, *A&A*, 400, 1021  
 Barraud C. et al., 2005, *A&A*, 440, 809  
 Belczynski et al., 2006, preprint (astro–ph/0601458)  
 Berger E., Kulkarni S.R., Frail D.A., 2003, *ApJ*, 590, 379  
 Berger E., Soderberg A.M., 2005, *GCN Circ.*, 4384  
 Berger E., et al., 2005, *Nature*, 438, 988  
 Berger E., 2005, *GCN Circ.*, 3801  
 Bloom J.S., Frail D.A., Kulkarni S.R., 2003, *ApJ*, 594, 674  
 Bosnjak Z., Celotti A., Longo F., Barbiellini G., 2006, preprint (astro–ph/0502185)  
 Bosnjak Z. et al., 2006, *A&A*, 447, 121  
 Borgonovo L., Bjornsson C.-I., 2006, preprint (astro–ph/0606487)  
 Burrows D.N. et al., 2005, *Science*, 309, 1833  
 Christensen L., Hjorth J., Gorosabel J., 2005, *ApJ*, 631, L29  
 Crew G.B. et al., 2003, *ApJ*, 599, 387  
 Crew G.B. et al., 2005, *GCN Circ.*, 4021  
 Crew G.B. et al., 2005, *GCN Circ.*, 3890  
 Cummings S. et al., 2005, *GCN Circ.*, 3479  
 Cusumano G., et al., 2006, *Nature*, 440, 164  
 D'Agostini G., 2005, preprint (physics/0511182)  
 Dado S., Dar A., 2004, *ApJ*, 627, L109  
 Dai Z. G., Liang E. W., Xu D., 2004, *ApJ*, 612, L101  
 Dai Z. G., Zang B., 2005, *ApJ*, 621, 875  
 Dar A., De Rujula A., 2004, *Phys. Rep.*, 405, 203  
 Donaghy T.Q., Graziani C., Lamb D.Q., 2005, *Nuovo Cimento C*, 28, 365  
 Donaghy T.Q., 2006, *ApJ*, 645, 436  
 Doty J., et al., 2005, *GCN Circ.*, 4145  
 Eichler D., Levinson A., 2004, *ApJ*, 614, L13  
 Fan Y.Z., Wei D.M., 2005, *MNRAS*, 364, L42  
 Fenimore E.E., et al., 2004, *GCN Circ.*, 2735  
 Firmani C., et al., 2006, preprint (astro–ph/0605073)  
 Fox D.B. et al., 2005, *Nature*, 437, 845  
 Frail D.A. et al., 2001, *ApJ*, 562, L55  
 Friedman A.S., Bloom J.S., 2005, *ApJ*, 627, 1  
 Frontera F., Antonelli, L.A., Amati L. et al., 2000, *ApJ*, 540, 697  
 Frontera F., Amati L., Costa E. et al., 2000, *ApJS*, 127, 59  
 Fynbo J.P.U. et al., 2004, *ApJ*, 609, 962  
 Gehrels N., et al., 2005, *Nature*, 437, 851  
 Ghirlanda G., Celotti A., Ghisellini G., 2003, *A&A*, 406, 879  
 Ghirlanda G., Ghisellini G., Lazzati D., 2004, *ApJ*, 616, 331  
 Ghirlanda G., Ghisellini G., Celotti A., 2004, *A&A*, 422, L55  
 Ghirlanda G., Ghisellini G., Lazzati D., Firmani C., 2004, *ApJ*, 613, L13  
 Ghirlanda G., Ghisellini G., Firmani C., Celotti A., Bosnjak Z., 2005, *MNRAS*, 360, L45  
 Ghirlanda G., Ghisellini G., Lazzati D., Firmani C., 2005, *Nuovo Cimento C*, 28, 303  
 Ghirlanda G., Ghisellini G., Firmani C., 2005, *MNRAS*, 361, L10  
 Ghisellini G., et al., 2006, *MNRAS*, preprint (astro–ph/0605431)  
 Granot J., Panaiteescu A., Kumar P., Woosley S.E., 2002, *ApJ*, 570, L61  
 Golenetskii S. et al., 2004, *GCN Circ.*, 2754  
 Golenetskii S. et al., 2005, *GCN Circ.*, 3179

Golenetskii S. et al., 2005, GCN Circ., 3518  
 Golenetskii S. et al., 2005, GCN Circ., 4150  
 Golenetskii S. et al., 2005, GCN Circ., 4238  
 Golenetskii S. et al., 2005, GCN Circ., 4394  
 Guidorzi C., et al., 2005, MNRAS, 363, 315  
 Guidorzi C., et al., 2006, preprint (astro-ph/0606526)  
 Kippen R.M., Woods P.M., Heise J. et al., 2001, in Costa E., Frontera F., Hjorth J. eds, Gamma-Ray Bursts in the Afterglow Era. Springer, Berlin Heidelberg, p.22  
 Hjorth J. et al., 2005, Nature, 437, 859  
 Jimenez R., Band D., Piran T., 2001, ApJ, 561, 171  
 Kaneko Y., Preece R.D., Briggs M.S., Paciesas W.S., Meehan C.A., Band D.L., 2006, preprint (astro-ph/0605427)  
 Krimm H. et al., 2005, GCN Circ., 3667  
 Lamb D.Q., Donaghy T.Q., Graziani C., 2004, NewAR, 48, 459  
 Lamb D.Q., Donaghy T.Q., Graziani C., 2005, ApJ, 620, 355  
 Levinson A., Eichler D., 2005, ApJ, 629, L13  
 Liang E.W., Dai Z.G., Wu X.F., 2004, ApJ, 606, L29  
 Liang E., Zhang B., 2005, ApJ, 633, 611  
 Lloyd N.M., Petrosian V., Mallozzi R.S., 2000, ApJ, 534, 227  
 Lloyd N.M., Petrosian V., 2002, ApJ, 565, 182  
 Lloyd-Ronning N.M., Dai X., Zhang B., 2004, ApJ, 601, L371  
 Longo F., Barbiellini G., Bosnjak Z.M., Celotti A., 2005, Nuovo Cimento C, 28, 689  
 Mastichiadis A., Kazanas D., 2006, ApJ, 645, 416  
 Mészáros P., 2002, ARA&A, 40, 137  
 Nakar E., Piran T., 2005, MNRAS, 360, L73  
 Nava L. et al., 2006, A&A, 450, 471  
 Norris J.P., Marani G.F., Bonnell J.T., 2000, ApJ, 534, 248  
 Norris J.P., Bonnell J.T., 2006, ApJ, 643, 266  
 Pedersen K., et al., 2005, ApJ, 634, L17  
 Pelangeon A. et al., 2006, AIPC, 838, 149  
 Perna R., Armitage P.J. & Zhang P., 2006, ApJ, 636, L29  
 Perri M. et al., 2005, A&A, 442, L1  
 Piran T., 2005, Rev. Modern Phys., 76, 1143  
 Pizzichini G. et al., 2006, preprint (astro-ph/0503264)  
 Preece R.D., Briggs M.S., Mallozzi R.S. et al., 2000, ApJS, 126, 19  
 Price P.A. et al., 2002, ApJ, 573, 85  
 Price P.A. et al., 2003, ApJ, 589, 838  
 Proga D., Zhang B., 2006, MNRAS, 370, L61  
 Ramirez-Ruiz E., 2005, MNRAS, 363, L61  
 Ramirez-Ruiz E. et al., 2005, ApJ, 625, L91  
 Reichart D.E. et al., 2001, ApJ, 552, 57  
 Reichart D.E., Nysewander M.C., 2006, preprint (astro-ph/0508111)  
 Rees M., Mészáros P., 2005, ApJ, 628, 847  
 Rossi E., Lazzati D., Rees M.J., 2002, MNRAS, 332, 94  
 Ryde F., 2005, ApJ, 625, L95  
 Sakamoto T. et al., 2004, ApJ, 602, 875  
 Sakamoto T. et al., 2005, ApJ, 636, L73  
 Sakamoto T. et al., 2005, ApJ, 629, 311  
 Sato R. et al., 2005, PASJ, 57, 6, 1031  
 Sato G. et al., 2005, GCN Circ., 3793  
 Sazonov S.Y., Lutovinov A.A., Sunyaev R.A., 2004, Nature, 430, 646  
 Schaefer B.E., 2003, ApJ, 583, L71  
 Soderberg A.M. et al., 2004, Nature, 430, 648  
 Tavani M., ApJ, 466, 768  
 Toma K., Yamazaki R., Nakamura T., 2005, ApJ, 635, 481  
 Ulanov M.V. et al., 2005, Nuovo Cimento C, 28, 351  
 Vaughan S. et al., 2006, ApJ, 638, 920  
 Villasenor J.S. et al., 2005, Nature, 437, 855  
 Watson D. et al., 2006, ApJ, 636, 967  
 Wu X.F. et al., 2006, preprint (astro-ph/0512555)  
 Xu D., Dai Z.G., Liang, E.W., 2005, ApJ, 633, 603  
 Yamazaki, R., Ioka, K., Nakamura, T., 2003, ApJ, 593, 941  
 Yamazaki, R., Yonetoku D., Nakamura, T., 2003, ApJ, 594, L79  
 Yamazaki, R., Ioka K., Nakamura, T., 2004, ApJ, 606, L33  
 Yonetoku D., Murakami T., Nakamura T. et al., 2004, ApJ, 609, 935  
 Zhang, B., Mészáros, P., 2002, ApJ, 581, 1236  
 Zhang B., Dai X., Lloyd-Ronning N.M., Mészáros P., 2004, ApJ, 601, L119